UNIVERSITY OF SOUTH BOHEMIA

FACULTY OF SCIENCE

Phenotyping of a Glutamate Dehydrogenase A Null Mutant of *Plasmodium falciparum*

Bc. JAN PERNER

Master Thesis

Supervisor: Prof. Sylke Müller - University of Glasgow

Supervisor specialist: Janet Storm, Ph.D. - Glasgow Biomedical Research Centre

České Budějovice

2011

Master Thesis

Perner, J., 2011: Phenotyping of a glutamate dehydrogenase a null mutant of *Plasmodium falciparum*. Mgr. Thesis, in English – 49 p., Faculty of Science, University of South Bohemia, České Budějovice, Czech Republic.

Annotation: Glutamate dehydrogenase a (GDHa) has been suggested as a potential drug target against the malaria parasite *Plasmodium falciparum*. GDHa knockout cell line was generated and needed a phenotypic description by means of molecular biology and biochemistry. The knockout cell line was tested for higher oxidative stress sensitivity, levels of relevant proteins and gene transcripts were quantified. Furthermore, concentrations of two key molecules enabling redox homeostasis, glutathione and NADPH, were attempted to quantify. Finally, we attempted to disrupt a gene of another glutamate dehydrogenase, *gdhb*, which did not result in formation of viable parasites. In conclusion, GDHa is not a suitable drug target and GDHb needs to be further elucidated.

This work was funded by Erasmus Programme based on a bilateral agreement 05/09/10/P.

I hereby declare that this thesis is based on my own work and all other sources of information have been acknowledged.

I hereby declare that, in accordance with Article 47b of Act No. 111/1998 in the valid wording, I agree with the publication of my master thesis, in full to be kept in the Faculty of Science archive, in electronic form in publicly accessible part of the STAG database operated by the University of South Bohemia in České Budějovice accessible through its web pages.

Further, I agree to the electronic publication of the comments of my supervisor and thesis opponents and the record of the proceedings and results of the thesis defence in accordance with aforementioned Act No. 111/1998. I also agree to the comparison of the text of my thesis with the Theses.cz thesis database operated by the National Registry of University Theses and a plagiarism detection system.

Date .....

Signature .....

Acknowledgments

I want to thank Professor Sylke Müller for giving me the opportunity to work and learn in her laboratory, for the opportunity to attend to the course of Molecular Biology and Biochemistry of Parasites, and last but not least for her always kind and helpful attitude towards me. I am grateful to Dr. Janet Storm for the overall guidance in the laboratory, introducing me into concise laboratory data recording, and for a good deal of patience through our experiment-design debates. Next, I want to thank Dr. Eva-Maria Patzewitz for HPLC assistance. Finally, I would like to thank Dr. Petr Kopáček for helpful suggestions during writing up.

Contents

1. Introduction

Being in the post genomic era, it is essential to assemble the gene products into their respective functional contexts. Even though there are various bioinformatics predictions, the ultimate identification of the function of a gene product can be achieved only by biochemical and molecular characterization (Ginsburg, 2009). Currently, there are 3151 gene products with unknown functions in the parasite *Plasmodium falciparum* out of 6372 predicted genes according to PlasmoDB (http://www.PlasmoDB.org; database version 7.1). The manual characterization of gene products with either unknown or predicted function is of highest importance.

Redox metabolism represents an intricate and important enzymatic network and as such can be considered as a potential drug target. The oxidoreductive enzymes of the redox network rely on organic prosthetic groups that serve as electron acceptors/donors. Two nicotinamide cofactors are utilised by the cell. First, nicotinamide adenine dinucleotide phosphate, NADPH, serves as a cofactor for several biosynthetic pathways and is a reductant of antioxidant and redox enzymes. Second, nicotinamide adenine dinucleotide, NAD(H), reflects mainly the energy state of the cell and enables energy gain in a respiratory chain. In addition to NAD(P)H, flavine adenine dinucleotide, $FAD(H_2)$, or lipoic acid are essential cellular cofactors. In the anabolic branch of metabolism, reductive forms of cofactors are used to donate electrons.

1.1. *P. falciparum* and malaria

Life cycle

P. falciparum is a parasitic protist that belongs to phylum Apicomplexa. This parasite is a causative agent of malaria in humans. The parasite has a very complex life cycle comprising of many specific stages (Fig. 1). *P. falciparum* undergoes an asexual part of its life cycle in humans and sexual part in insect vectors which are, by definition, the main host of the parasite. As the parasite needs to survive in various dissimilar environments for a relatively short period of time, it needs to undergo very rapid and specific changes.

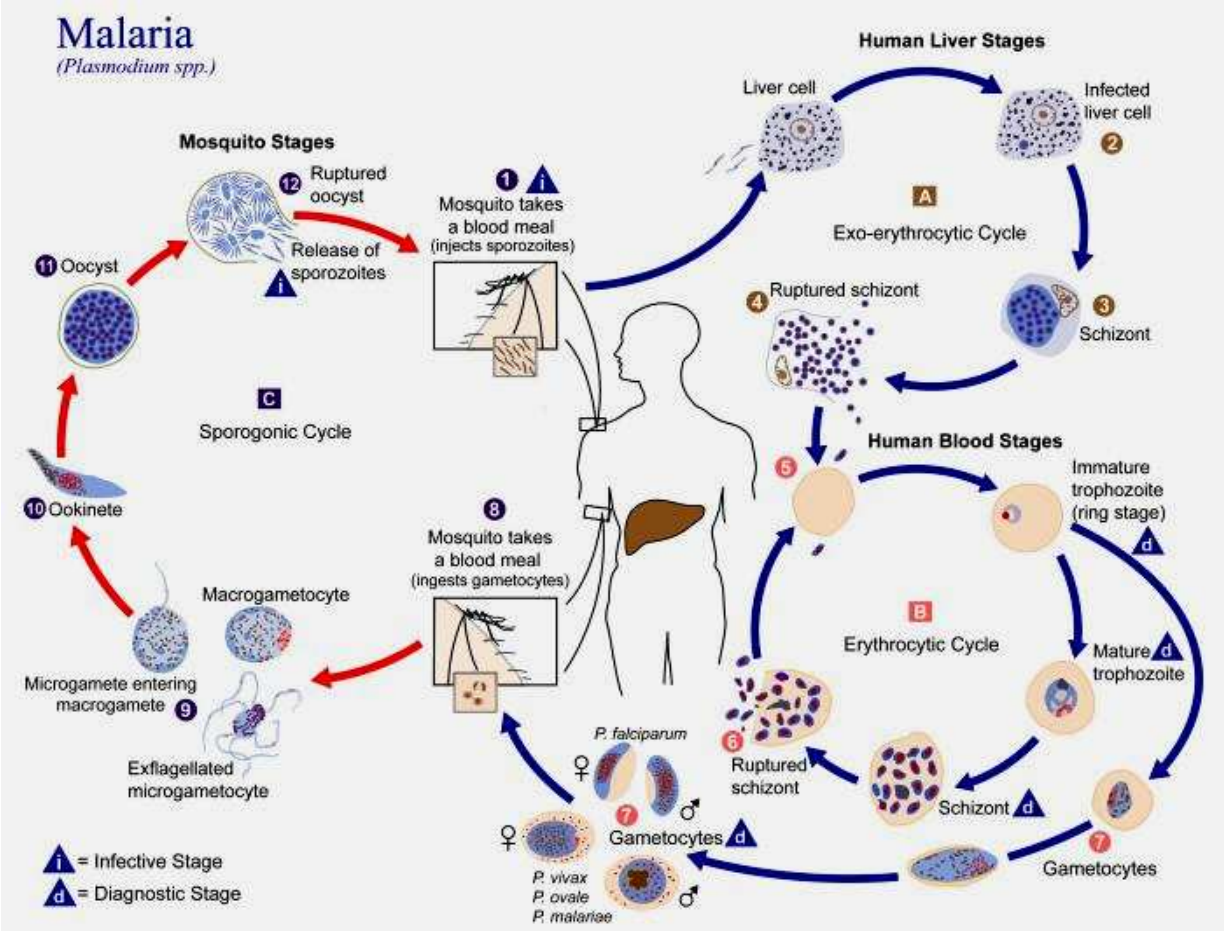

Figure 1. The life cycle of *Plasmodium* sp. When *Plasmodium*-infected mosquito takes a blood meal, it injects sporozoites in the human bloodstream. The sporozoites infect liver cells, develop and differentiate into merozoites that are released in the bloodstream. The merozoites invade red blood cells where they mature into trophozoites and schizonts that eventually release merozoites upon rupture. Some trophozoites develop into gametocytes that are infective to the mosquito. In mosquito gut, the gametocytes develop into gametes that mate with each other to form a zygote. The zygote differentiates into an ookinete that traverses the mosquito midgut epithelium and matures into an oocyst. After the oocyst development, the oocyst releases sporozoites that migrate to salivary glands and the life cycle is completed (courtesy of CDC/Alexander J. da Silva, PhD/Melanie Moser).

Human stages

The human life cycle commences with the injection of sporozoites into the host skin. Once the sporozoites enter the skin, they rush to the liver to infect hepatocytes and mature and asexually multiply into thousands of infective cells called merozoites. This is not true for all *Plasmodium* species. It has been recently shown by *in vivo* real-time imaging experiments with *P. berghei* in rodents that half of the sporozoites may remain in the epidermis and either persist there or differentiate into infective cells omitting thus the liver stage (Gueirard et al., 2010). The sporozoites of *P. falciparum*, at the current state of knowledge, travel through the bloodstream into liver cells where they mature into merozoites and multiply up to tens of thousands merozoites and these merozoites enter the bloodstream. The merozoites

actively invade red blood cells (RBCs) and upon RBC invasion, the merozoites are held within parasitophorous vacuole where they undergo further differentiations. There are two possible scenarios:

a) The parasites mature into a ring stage and then further into trophozoites and schizonts; from one merozoite invading a RBC, up to 32 daughter merozoites are generated through schizogonic replication. The daughter merozoites are released into the bloodstream where they invade new RBCs and a new asexual replication cycle commences. This release of merozoites causes the clinical manifestation of malaria.

b) To sustain a transmission, a small percentage of the blood stages stop multiplying by mitotic (asexual) division and instead differentiate into sexual cells, gametocytes. The gametocytes circulate in the peripheral blood in a state of developmental arrest. These stages are infective to the mosquito where they receive signals to transform into micro- and macrogametes (Kuehn and Pradel, 2010).

Mosquito stages

Anopheles mosquito, if fed on a malarial patient, takes up infected RBCs together with a blood meal. Once taken up, gametocytes leave RBCs and develop into gametes in the mosquito midgut. The gametes are of two types: male (microgamete) and female (macrogamete). One female gametocyte give rises to one macrogamete in contrast to a male gametocyte giving rise to 8 flagellar motile microgametes. This mechanism explains the disproportional (more female gamotocytes) occurrence of male and female gametocytes in the blood samples of malaria patients (Schall, 1989). The resulting gametes then mate together forming a zygote. The zygote then develops into a motile cell, ookinete, that traverses a midgut and becomes an oocyst. The oocysts reside at the basal lamina of the midgut where they undergo multiplications creating new sporozoites. These sporozoites asynchronously leave the oocyst and travel through haemolymph to finally invade salivary glands.

Morphologic description

As mentioned above, *P. falciparum* belongs to phylum Apicomplexa and as such possesses several peculiar organelles. In the apical pole, *Plasmodium* spp. have apical complex of organelles, hence the name of the phylum. This complex facilitates active invasion of the parasite into host cells. The complex consists of dense granules, micronemes, and rhoptries. *Plasmodium* spp. retained a vestigial plastid, an apicoplast. Even though the apicoplast has

lost its photosynthesis-related genes, it harbours many essential metabolic pathways such as mevalonate independent 1-deoxy-D-xylulose 5-phosphate (DOXP) pathway to synthesise isoprenoids, type II fatty acid synthesis (FAS II), and a part of haem synthesis (Seeber and Soldati-Favre, 2010).

Apart from these peculiarities, the parasite, possesses some of the more common and ubiquitous organelles. Food vacuole, for instance, is an organelle where proteolytic digestion of ingested red blood cell haemoglobin takes place supplying the parasite with most amino acids (Cobbold et al., 2011). Next, the food vacuole is responsible for detoxification of haem whereby the soluble haem molecule is biocrystallised into insoluble haemozoin molecules (Loria et al., 1999). Incidentally, the essentiality of this organelle and of the reactions taking place within was reflected by significant therapeutic success of chloroquine treatments in the latter half of the last century (Slater and Cerami, 1992). In addition, the parasites possess a single mitochondrion, a nucleus, endoplasmatic reticulum and Golgi apparatus.

Malaria

Malaria is one of the most devastating diseases besetting the current humankind. Malaria causes more than a million human deaths each year. Especially in Africa, malaria takes a heavy toll on human welfare. According to WHO (http://www.WHO.int; report from 2009), every fifth child dies due to the effects of the disease in Africa. Apart from Africa, malaria threatens tropical and subtropical regions in both Asia and South America. It is notable that more than a half (51%) of the world's estimated *P. falciparum* clinical cases are located in just four countries: India, Nigeria, Democratic Republic of the Congo, and Myanmar (Hay et al., 2010).

Glucose-6-phosphate dehydrogenase deficiency

Glucose-6-phosphate dehydrogenase (G6PDH) deficiency is an X-chromosome-linked genetic disorder. Four hundred million people worldwide carry one or two deficient G6PD genes, making G6PD deficiency the most common enzyme pathology (Peters and Van Noorden, 2009).

G6PD of red blood cells catalyses the first step of the hexose-monophosphate shunt (HMS) which supplies pentoses to further biosyntheses and regenerates NADPH. Even though the human RBCs have a limited need for nucleotides and reducing power, impairment of this step makes the RBCs vulnerable to oxidative damage by preventing glutathione disulphide

reduction. The RBC is demonstrably under oxidative stress when infected by *Plasmodium* parasites (Friedman, 1979; Hunt and Stocker, 1990). The oxidative stress mainly stems from digestion of host cell cytosol inside the acidic food vacuole of the parasite (Atamna and Ginsburg, 1993). Furthermore, the growth of *P. falciparum* has been found to be retarded in G6PDH-deficient RBCs (Roth et al., 1983). It is thus generally accepted that malaria has been a major selective pressure for the spread of the deficiency. High prevalence of G6PD deficiency is therefore common in past and present malaria endemic areas (Yoshida and Roth, 1987).

1.2. Antioxidant system and oxidative stress

Antioxidant defence can be divided into five categories: a) avoidance, b) antioxidant enzymes, c) free-radical scavengers, d) repair mechanisms, e) stress responses (Lane, 2002). While some organisms, particularly those that hide from oxygen like methane-producing or sulphate-reducing bacteria, rely mainly on the avoidance, *Plasmodium* sp., or many other organisms that are exposed to oxygen need to utilize the whole arsenal of antioxidant enzymes and low molecular weight scavengers to prevent oxidative damage to their macromolecules caused by oxygen intermediate species collectively named reactive oxygen species (ROS). The parasite evolved means how maintain hydrogen peroxide and superoxide radicals at relatively constant intracellular steady-state concentrations (Turrens, 2004). These two ROS are not highly reactive and harmful but become particularly detrimental in the presence of metals such as iron which can catalyse the formation of hydroxyl radicals that are ferociously reactive and, by contrast to superoxide and hydrogen peroxide, cannot be eliminated by cellular antioxidants (Lane, 2002). Going through an intraerythrocytic stage, the parasite metabolizes high amounts of oxygen (forming hydrogen peroxide) and iron (Turrens, 2004), the prerequisites for hydroxyl radicals generation. The reaction between hydrogen peroxide and iron is called the Fenton reaction:

$$H_2O_2 + Fe^{2+} \rightarrow OH^- + {}^{\bullet}OH + Fe^{3+}$$

Moreover, upon haemoglobin digestion, another harmful species is formed. Toxic haem (ferri/ ferroprotoporphyrin IX; FP IX) is released and since FP IX is damaging cellular macromolecules, it must be detoxified. Up to 90% of FP IX is biocrystallised (Egan et al., 2002) to form inert haemozoin. The antioxidant system represents a very complex evolutionary network and harbours essential ways for the parasite to survive in the RBC and

that is why this system has been intensely studied with a vista for finding and validating exploitable drug targets.

Antioxidant enzymes

Two of the most important antioxidant enzymes are superoxide dismutase and catalase. Virtually every organism that spends any time in the presence of oxygen needs to encode for these two enzymes. A rare exception is *P. falciparum* that possesses no catalase but contains two superoxide dismutases (SOD). SOD catalyses the dismutation of superoxide releasing hydrogen peroxide and oxygen. As the parasite lacks catalase it must have evolved another way to reduce hydrogen peroxide. This catalysis was attributed to small enzymes called peroxiredoxins (Kawazu et al., 2000). Moreover, peroxiredoxins seem to have taken over the antioxidant role of catalase in many other parasites like *Fasciola hepatica, Schistosoma mansoni,* and *Trypanosoma cruzi* (McGonigle et al., 1997; Kwatia et al., 2000; Wilkinson et al., 2000).

Superoxide dismutases

The front line of this enzymatic arsenal constitutes superoxide dismutases (SOD). Metallo-proteins that catalyse the dismutation of superoxide radicals. Superoxide radical is an oxygen intermediate with one unpaired electron. Having an unpaired electron, superoxide is fairly reactive damaging lipids, DNA, and proteins. SODs dismutate superoxide radicals to hydrogen peroxide and oxygen with the aid of incorporated metals in their active sites. The incorporation of metals into proteins aids to lead the oxidative reaction in a specific manner and thus circumvent unwanted side reactions. The parasite possesses two SODs, cytosolic SOD1 (PF08_0071) bearing Fe^{3+} and SOD2 (PFF1130c) that is also iron-dependent. SOD2 is targeted to apicoplast/mitochondrion during intraerythrocytic stages of the parasite (Sienkiewicz et al., 2004; Pino et al., 2007).

Peroxiredoxins

Peroxiredoxins are non-haem peroxidases that catalyse the reduction of hydrogen peroxide to water and concomitant oxidation of their cysteine thiols to sulphenic acid. These enzymes are widespread and fairly abundant (Bernroitner et al., 2009). In red blood cells, for example, peroxiredoxin 2 is one of the most abundant proteins after haemoglobin (Manta et al.,, 2009). Even though the reduction of this peroxiredoxin 2 occurs very slowly in the red blood cell, its high abundance and substrate specificity allow the peroxiredoxin 2 to act as a

non-catalytic scavenger of hydrogen peroxide (Low et al., 2007). Peroxiredoxins can be divided into 3 categories based on number of cysteines that are involved in the catalysis: typical 2-Cys peroxiredoxins, atypical 2-Cys peroxiredoxins, and 1-Cys peroxiredoxins. *P. falciparum* encodes 3 peroxiredoxins, two of which are typical 2-Cys peroxiredoxins and the third one is a 1-Cys peroxiredoxin. One of the 2-Cys peroxiredoxins (PF14_0368) and the 1-Cys peroxiredoxin (PF08_0131) are cytosolic, while the other 2-Cys peroxiredoxin (PFL0725w) possesses a mitochondrial targeting peptide (Boucher et al., 2006). Another peroxiredoxin was recently shown to associate with the nucleus of the parasite (Richard et al., 2011). It is thought that the cytosolic 2-Cys peroxiredoxin represents a key antioxidant in the parasite (Akerman and Müller, 2003). However, it was shown not to be essential for the parasite survival (Yano et al., 2008) suggesting a certain degree of redundancy of the antioxidant systems of the parasite.

Glutathione redox system and glutathione-based detoxification

Glutathione is a tripeptide comprised of L-glutamate, L-cysteine, and glycine. Its biosynthesis is carried out in two consecutive ATP-dependent steps. The first step is catalysed by γ-glutamylcysteine synthetase (PFI0925w) which ligates the amino group of cysteine to γ-carbon of the second carboxy group of glutamate to form a so called isopeptide bond. This catalysis is the rate limiting step of the synthesis of GSH. The second step is catalysed by glutathione synthetase (PFE0605c) when glycine is added to the dipeptide. GSH synthesis takes place in the cytosol. GSSG reduction is not only confined to the cytosol but was also found to be located in the apicoplast; glutathione reductase (PF14_0192) appears to be dually located through alternative transcriptional initiation in both cytosol and apicoplast (Kehr et al., 2010). Apart from that, glutathione may be conjugated to toxic chemicals via glutathione S-transferase (PF14_0187) rendering the chemicals harmless. Furthermore, the parasite possesses a functional glutathione-dependent glyoxalase system comprising of two enzymes glyoxalase I (PF11_0145) and glyoxalase II (PFD0311w) (Akoachere et al., 2005) to guard the parasite from reactive aldehydes.

Thioredoxin redox system

Thioredoxin is a low-molecular-weight peptide that co-maintains the redox homeostasis of the parasite. *P. falciparum* encodes for three thioredoxins, thioredoxin 1 localizes to the cytosol, thioredoxin 2 localizes to parasitophorous vacuole and potentially also to the mitochondrion, and thioredoxin 3 localizes to rough endoplasmatic reticulum (Boucher et

al., 2006; de Koning-Ward et al., 2009; Kehr et al., 2010). Thioredoxins are reduced by the thioredoxin reductase, a homodimeric NADPH dependant enzyme that has a dual location in cytosol and mitochondrion, respectively (Kehr et al., 2010). Furthermore, *P. falciparum* possesses a whole myriad of small proteins belonging to the thioredoxin super family [thioredoxins (Trx 1, 2, 3; thioredoxin-like proteins (Tlp 1, 2); glutaredoxin (Grx); glutaredoxin-like proteins (Glp 1, 2, 3); plasmoredoxin (Plrx)] that serve as a redox messengers and interact with redox active proteins and metabolites such as ribonucleotide reductase, transcription factors, peroxidases, or low-molecular-weight thiols.

Glyoxalase system

Glyoxalase system represents next important set of reactions to defend the cells from the free radicals. The parasite energy gain basically relies on glucose catabolism. Since glycolytic net gain is only 2 ATP moles/mole of glucose, the parasite needs to consume huge amounts of glucose to keep itself alive. Accordingly, the production of electrophilic 2-oxoaldehydes is thought to be increased because they are formed as side products of several metabolic pathways with glycolysis being the prime source. The glyoxalase system constitutes a glutathione- (i.e. NADPH-) dependent intracellular pathway converting toxic 2-oxoaldehydes, such as methylglyoxal, to the corresponding 2-hydroxyacids. The complete glyoxalase system has been described in *P. falciparum* and due to a uniqueness of one part of the system plus the postulation that inhibition of such a system would be detrimental only for the parasite, it has been suggested as a potential drug target (Akoachere et al., 2005).

1.3. Cellular redox systems

The tightly controlled maintenance of the intracellular redox environment is crucial for normal cellular functions. The redox state of a cell (Fig. 2) is mediated by the ratios of reduced and oxidised pyridine nucleotides [$NAD(P)H/NAD(P)^+$] and thiols such as glutathione/glutathione disulphide (GSH/GSSG) and thioredoxin/thioredoxin disulphide [$Trx(SH)_2/Trx(S)_2$] (Müller, 2004). These systems do not have to be maintained only in the cytosol but also in the organelles like mitochondrion or apicoplast. In *Toxoplasma gondii*, for example, $NADP^+$-dependent isocitrate dehydrogenase provides reducing equivalents in both mitochondrion and apicoplast (Pino et al., 2007).

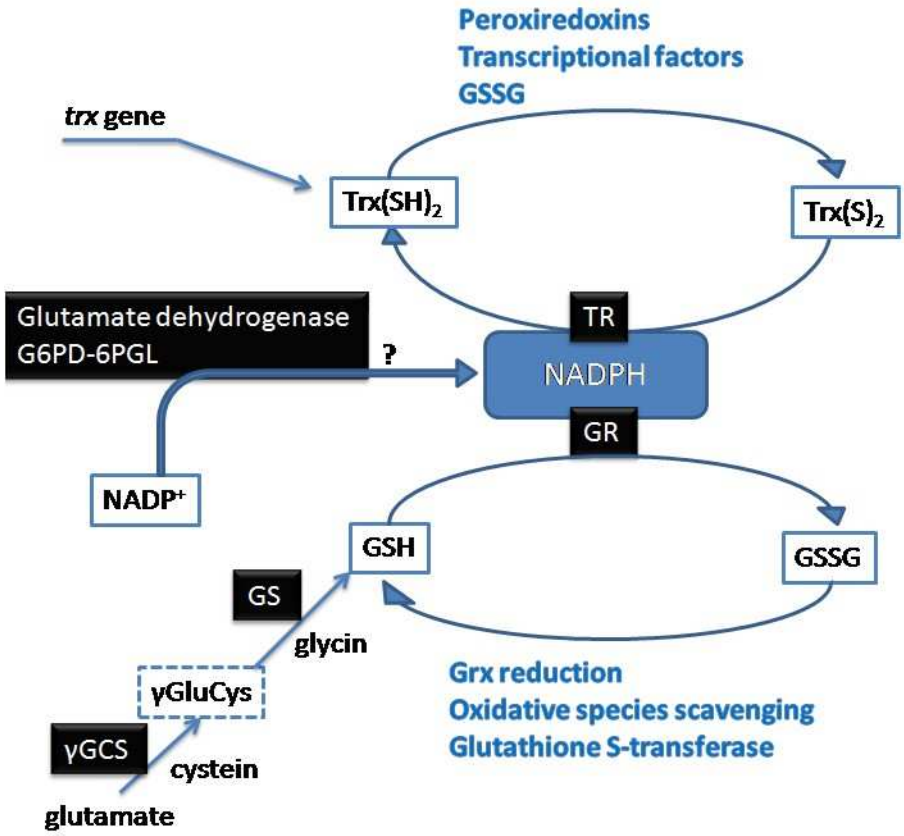

Figure 2. Depiction of NADPH utilization in redox cycles. NADPH serves as a reductant for both glutathione reductase (GR) and thioredoxin reductase (TR). TR reduces cytosolic thioredoxin disulphide [$Trx(S)_2$] to thioredoxin [$Trx(SH)_2$], while GR reduces glutathione disulphide (GSSG) to glutathione (GSH). Thioredoxin reduces peroxiredoxins, transcriptional factors, or can reduce glutathione disulphide non-enzymatically. GSH reduces glutaredoxins (Grx) or is used by glutathione S-transferase to label electrophiles for degradation or excretion. GSH also acts as reducing cofactor for GSH-dependent peroxidases. Thioredoxin is a product of a gene PF14_0545. Glutathione needs to be synthesised in two consecutive enzymatic steps. Cysteine and glutamate are ligated via catalysis of γ-glutamylcysteine synthetase (γGCS) and glycine is then ligated to γ-glutamylcysteine dipeptide via glutathione synthetase (GS). In order to recycle GSH from GSSG or [$Trx(SH)_2$] from [$Trx(S)_2$], the reducing cofactor NADPH is required. Normally, this is provided by glucose-6-phosphate dehydrogenase but other NADPH generating proteins such as isocitrate dehydrogenase or glutamate dehydrogenase may also play an important part in providing NADPH for reductive reactions. These enzymes are also present in the malaria parasite *P. falciparum* with isocitrate dehydrogenase being mitochondrial. In *P. falciparum*, glucose-6-phosphate dehydrogenase is fused with 6-phosphogluconolactonase forming a bifunctional enzyme glucose-6-phosphate dehydrogenase-6-phosphogluconolactonase (G6PD-6PGL, PF14_0511).

NADPH-generating pathways in *P. falciparum*

NADPH can be regarded as a fundamental reducing species for sustaining an antioxidant system of the cell (as reducing cofactor of thioredoxin- and glutathione disulphide). Apart from that, NADPH plays a vital role in biosynthetic pathways such as fatty acid and

isoprenoid biosynthesis or deoxyribonucleotide formation. In most animal cells, NADPH is regenerated in the oxidative branch of hexose-monophosphate shunt (HMS) (Roth, 1990). This reaction is, in most organisms, catalysed by glucose-6-phosphate dehydrogenase (G6PDH). It was long thought that *P. falciparum* does not possess G6PDH and was thus considered disabled to produce its own NADPH (Vander Jagt et al., 1989). Parasite G6PDH activity was first detected in the parasites isolated from G6PDH-defficient patients where the parasite G6PDH is activated to cover the NADPH demand (Usanga and Luzzatto, 1985). The parasite G6PDH was then characterized and it was noted that its activity accounts for 90% of G6PDH activity in G6PDH-defficient patients but it still does amount to as little as 5% of normal red blood cell G6PDH activity (Yoshida and Roth, 1987). Similarly, it was noted that parasite G6PD activity is of no more than 10% of normal red blood cell G6PDH activity (Ling and Wilson, 1988). It was also shown by GSSG reduction potency that, in addition to G6PDH-mediated NADPH production in G6PDH-defficient RBCs, the parasitised normal RBCs reduce more GSSG over control only via glutamate dehydrogenase catalysis (Roth et al., 1986). In contrast to these results, Ginsburg and colleagues noted that the HMS activity of *P. falciparum* is 78 times higher even in infected normal red blood cells than in normal red blood cells, 82% of which is contributed to the parasite HMS activity (Atamna et al., 1994). It is now known that the first two steps of HMS pathway in *P. falciparum* are catalysed by one bifunctional enzyme, glucose-6-phosphate dehydrogenase-6-phosphogluconolactonase (PF14_0511) (Clarke et al., 2001). The recombinant enzyme has been recently characterised but the question of NADPH contribution *in vivo* was not addressed (Jortzik et al., 2011). Due to low parasite G6PDH activity (Roth et al., 1986; Yoshida and Roth, 1987; Ling and Wilson, 1988), alternative pathways for NADPH production were sought for. Vander Jagt and colleagues purified and characterised two other possible NADPH-generating enzymes: glutamate dehydrogenase (GDH) and $NADP^+$-specific isocitrate dehydrogenase (IsoDH) finding that GDH can produce about 10% and IsoDH 20–60% of normal red blood cell NADPH capacity (Vander Jagt et al., 1989). The IsoDH activity increases with the parasite maturation. The activity of IsoDH indicated that this enzyme might offer more NADPH than GDH (Vander Jagt et al., 1989). However, it was later experimentally proven that the IsoDH is located in the mitochondrion (Olszewski et al., 2010) so it is not likely that this enzyme would provide NADPH for the cytosolic metabolism unless the parasite contains a mechanism to transfer reducing equivalents from mitochondrion to cytosol. Such a mechanism may be facilitated by transhydrogenases as in *Hymenolepis dismuta* (Mercer-Haines and Fioravanti, 2008). The possibility that NADPH of

the host cell is available for the parasite to salvage it and use has been suggested for *P. berghei* (Eckman and Eaton, 1979). However, it is not clear if the host NADPH is available for *P. falciparum*.

It is surprising that more than twenty years after these experiments, there is very little known as to how the parasite maintains its NADPH pool in both cytosol and organelles. Therefore the role of one of the three glutamate dehydrogenases present in the malaria parasite *P. falciparum,* glutamate dehydrogenase a, in maintenance of the parasites reducing homeostasis was assessed in this thesis.

Glutamate dehydrogenase

Glutamate dehydrogenases are ubiquitous enzymes that represent an important link between nitrogen and carbon metabolism. They catalyse the reversible NAD^+ or $NADP^+$-dependant oxidative deamination of L-glutamate to 2-oxoglutarate and ammonia.

$$\text{L-glutamate} + H_2O + NAD(P)^+ \leftrightarrow \text{2-oxoglutarate} + NH_4^+ + NAD(P)H$$

In plants and bacteria, NAD^+-dependent glutamate dehydrogenases are involved in glutamate deamination, and NADPH-dependant are known to be involved in ammonia fixation on 2-oxoglutarate (Purnell and Botella, 2007; Harper et al., 2010). In mammals, the enzyme can utilise either cofactor and is important for the deamination of L-glutamate (Plaitakis and Zaganas, 2001). In *P. falciparum,* $NADP^+$-dependent glutamate dehydrogenase was first identified by Krauth-Siegel and colleagues (1996). In 1998, the same group characterised the recombinantly expressed protein and showed that the enzyme catalyses both the deamination of L-glutamate and the amination of 2-oxoglutarate (Wagner et al. 1998). Because of a relatively low affinity for ammonia (K_m values of 7–10 mM) it was suggested that the enzyme primarily supports the deamination of L-glutamate thus providing NADPH for reductive reactions and 2-oxoglutarate that may be metabolized in the tricarboxylic acid pathway (Wagner et al., 1998). When the parasite genome was unveiled, three GDH genes were predicted (Table 1).

Enzyme	PfID	Molecular weight	Coenzyme specificity	Cell localization
GDHa[1]	PF14_0164	50 kDa *	$NADP^+$-dependent*	cytosolic*
GDHb	PF14_0286	57 kDa	$NADP^+$-dependent	apicoplast
GDHc	PF08_0132	160 kDa	unknown	unknown

Table 1. Glutamate dehydrogenase (GDH) enzymes encoded in *P. falciparum* genome. They are listed by their abbreviations, together with their gene identification (PfID) in the *Plasmodium* genome database (www.PlasmoDB.org), calculated/*experimentally determined molecular weight, predicted/*experimentally determined coenzyme specificity, and predicted/*experimentally determined subcellular localization of predicted proteins.

1.4. Carbon metabolism

P. falciparum blood stages do not exhibit oxidative phosphorylation and therefore the glycolytic pathway constitutes the main energy source for the parasite (van Dooren et al., 2006). The major end product of this pathway, apart from more conventional phospho*enol*pyruvate which is then predominantly dephosphorylated to pyruvate and reduced to lactate by lactate dehydrogenase (Sherman, 1979), was identified to be glycerol (Lian et al., 2009). Lactate dehydrogenase is an essential enzyme for the parasite as it maintains the NAD^+ flux for the glycolytic pathway without which would the glycolysis ceases (Ginsburg, 2002).

A central hub of carbon metabolism is the tricarboxylic acid cycle which connects the processes of glycolysis, gluconeogenesis, respiration, amino acid synthesis/degradation, and other biosynthetic and catabolic pathways. In most organisms, the tricarboxylic acid metabolism constitutes a cyclic pathway. In *P. falciparum*, however, the pathway has a branched structure (Fig. 3) in which the major carbon source comes from the amino acids glutamate and glutamine (Olszewski et al., 2010). Pyruvate dehydrogenase, an enzymatic complex usually localized in the mitochondrion, catalyses the formation of acetyl coenzyme A (acetyl-CoA). In *Plasmodium* sp., however, the complex is localized in the apicoplast (Foth et al., 2005) and even though it produces acetyl-CoA, it does not seem to be provided for the mitochondrion. Instead it is used to generate fatty acids (Pei et al., 2010) and to provide acetyl groups for the acetylation of histones and amino sugars (Olszewski et al., 2010). One of the two $NADP^+$-dependent glutamate dehydrogenases is thought to not only provide NADPH but also constitutes a gate keeper controlling how much of 2-oxoglutarate

[1] GDHa is the GDH that was previously described in literature.

is made and thus co-controlling how much of this metabolite is fed into the parasite's TCA pathway where it is either further oxidized or reduced (Mogi and Kita, 2010; Olszewski et al., 2010).

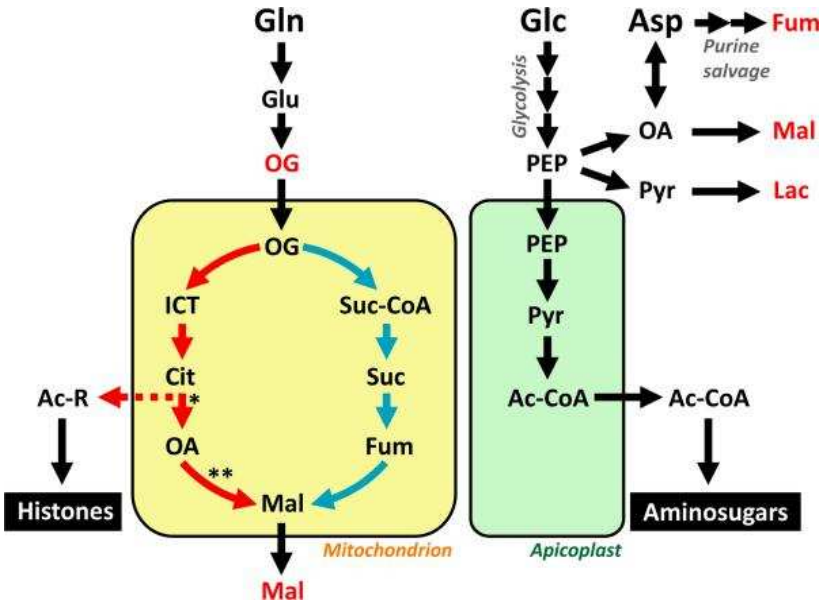

Figure 3. Branched architecture of TCA metabolism in *P. falciparum*. Several reactions run in the reverse of the standard direction, these reactions are reductive and are indicated by red arrows. It further depicts two different biological fates of glutamine-derived and glucose-derived acetyl-CoA. Phospho*enol*pyruvate (PEP) is converted to pyruvate (Pyr) and oxaloacetate (OA) in the cytosol. Cytosolic oxaloacetate is interconverted to aspartate (Asp) by aspartate aminotransferase. Aspartate can be then used, for instance, in a purine salvage machinery where a fumarate (Fum) is formed as a byproduct. All metabolites in red are effluxed into the media as waste products. Taken from: Olszewski et al., 2010; permission granted by Nature Publishing Group.

The oxidative arm of the TCA metabolism generates succinyl-CoA, NADH, and CO_2 via the 2-oxoglutarate dehydrogenase complex. Much like the pyruvate dehydrogenase complex, the 2-oxoglutarate dehydrogenase complex is composed of three subunits (Foth et al., 2005). Similarly, the enzyme complex responsible for the degradation of branched chain α-keto acids derived from the branched chain amino acids valine, leucine, and isoleucine, is the branched-chain α-keto acid dehydrogenase (BCKDH) complex. The E2 transacylase subunits (E2 subunit) of all three α-keto acid dehydrogenase complexes (KADH) display a lipoic acid cofactor specificity (Günther et al., 2007). The KADH complexes are localized in both/either the mitochondrion and/or the apicoplast and each organelle possesses its own lipoylation pathways which were suggested as excellent potential drug targets (Günther et al., 2005, 2009 a, b).

2. Material and Methods

Abbreviations

BSA	bovine serum albumine
CDC	Center for Disease Control and Prevention
DTPA	diethylenetriamine penta-acetic acid
EBSS	Earle's balanced salt solution with phenol red
EPPS	3-[4-(2-hydroxyethyl)piperazin-1-yl]propane-1-sulphonic acid
GSH	reduced form of glutathione
GSSG	glutathione disulphide
HRP	horseradish peroxidase
NTC	no template control
PBST	PBS + 0.5% Tween
PMS	N-methylphenazonium methosulphate
RBC	red blood cell
RT	room temperature
SDS	sodium dodecyl sulphate
t-BuOOH	*tert*-butyl hydroperoxide
TCA	tricarboxylic acid
TCEP	tris(2-carboxyethyl)phosphine

Media and solutions

Complete RPMI 1640 medium	15.9 g/l RPMI 1640 (with L-glutamine and 25 mM HEPES), 0.5% Albumax II, 0.1% $NaHCO_3$, 200 µM hypoxanthine, 20 mg/l gentamicine, pH 7.4
Incomplete RPMI 1640 medium	15.9 g/l RPMI 1640 (with L-glutamine and 25 mM HEPES), 0.1% $NaHCO_3$, 200 µM hypoxanthine, 20 mg/l gentamicine, pH 7.4
IC_{50} medium	15.9 g/l RPMI 1640 (with L-glutamine and 25 mM HEPES), 0.5% Albumax II, 0.1% $NaHCO_3$, 20 mg/l gentamicine, pH 7.4
Cytomix	120 mM KCl, 0.15 mM $CaCl_2$, 2 mM EGTA, 5 mM $MgCl_2$, 10 mM K_2HPO_4 / KH_2PO_4, 25 mM HEPES pH 7.6
Electrophoretic Buffer (SDS-PAGE)	25 mM Tris, 192 mM Glycine, 0.1% SDS
Extraction Buffer (NADPt extraction)	20 mM $NaHCO_3$, 100 mM Na_2CO_3, 0.1% Triton X-100
Lysis Buffer (protein preparation)	0.5% Triton X-100 in PBS, protease inhibitors: 1 mM PMSF, 1 mM benzamidine, 20 µM leupeptin, 10 µM E-64, 2 µM 1.10-phenantroline, 4 µM pepstatin A
Reducing Buffer (GSSG reduction)	40 mM EPPS, 4 mM DTPA, 700 µM TCEP, pH 8.0 (LiOH)
Towbin Buffer - stock solution 10x 20%	25 mM Tris, 192 mM Glycine, 1.3 mM SDS, methanol
Towbin Buffer - working solution 1x	1:2:7 (10x Towbin Buffer : methanol : water)
Sorbitol solution	sorbitol dissolved in 10 mM potassium phosphate pH 7.2

2.1. Maintenance of *Plasmodium falciparum* in *in vitro* cultures

The *Plasmodium falciparum* (*P. falciparum*) culture was kept in RPMI 1640 complete medium with human erythrocytes at 5% haematocrit. Human blood was obtained from Glasgow Blood Transfusion Services. The blood was washed several times in incomplete RPMI 1640 medium and the resulting pellet was stored in fridge for up to a month. The cultures were maintained in an atmosphere with reduced oxygen (96% N_2, 3% CO_2, 1% O_2) at 37 °C. All work with live cultures was carried out in a suite designated for work with agents of biohazard level 3 on a CDC scale. All media and chemicals used for culturing were filter sterilised through a 0.22 µm filter.

Parasites with a knocked out gene or a transfected plasmid had to be maintained under a selective pressure of drugs like WR99210 or blasticidin-S. These drugs were kept at constant concentrations and were exchanged on a daily basis together with medium exchange.

2.2. D10 *in vitro* cycle

There are numerous aspects that vary not only amongst *Plasmodium* species but also amongst strains of the same species. To name but a few: there are various ratios of blood stages switching to gametocytes differentiation, there are various numbers of merozoites formed within one schizont, resistance to diverse drugs, the timing of particular stages differs substantially, and so forth. D10 is an isolate from Papua New Guinea and its intrinsic characteristic is that it does not form any gametocytes in the culture so it is a suitable strain to work with to investigate intraerythrocytic stages. D10 schizonts form usually five merozoites/schizont. The merozoites first develop into an early ring stage (0–8 h), followed by rings (8–16 h) and finally late rings (16–24 h). The late rings develop into early trophozoites (24–26 h), trophozoites (26–36 h), late trophozoites (36–40 h), and at the end they mature into schizonts (40–48 h) which then release merozoites again (Fig. 4).

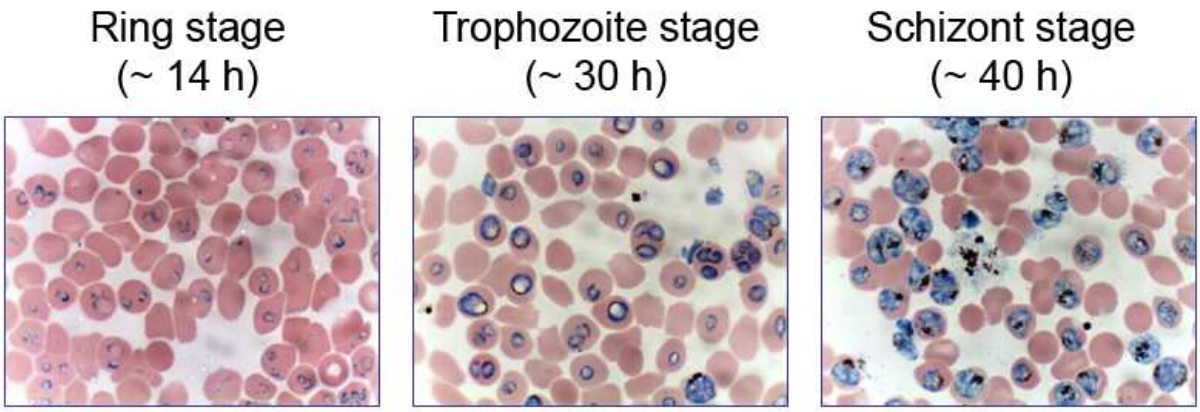

Figure 4. Wright-stained synchronised culture of *P. falciparum*. First picture captures synchronised ring culture after around 14 hours after invasion of merozoites in the red cells. Middle picture depicts trophozoite stage after about 30 hours post merozoite invasion. Small haemozoin particles are already visible (the brown grains). The right picture captures schizont stages just before the rupture and merozoite egress. Haemozoin constitutes already quite big particles. Taken from: Radfar et al., 2009; permission granted by Nature Publishing Group.

2.3. Blood smears and microscopy

To inspect the culture, determine the parasitaemia, or to determine the stage of parasites, blood smears were made. A thin even film was made from a 5 µl-drop of sedimented RBCs on a slide. The smear was airdried, methanol-fixed, and Giemsa-stained. The smear was then observed under a light microscope (Pyser-SGI) under 100x objective magnification.

2.4. Parasite stabilates

Parasite cultures that were not in use were kept in liquid nitrogen as a stabilate. Stabilates were made from a culture of 5% parasitaemia. Infected RBCs were pelleted at 800 × g for 5 min at 4 °C. The pellet was resuspended in one pellet volume of ice cold RPMI 1640 complete medium. Two pellet volumes of freezing solution (30% glycerol in PBS) were then added. The resulting suspension was carefully mixed, aliquoted out into cryotubes, and frozen in liquid nitrogen.

2.5. Parasite stabilates defrosting

The stabilates were immediately transferred on ice once taken out of liquid nitrogen. The stabilate was placed in a water bath (37 °C) for a few seconds and then returned on ice. The cells were resuspended in two volumes of ice cold 27% sorbitol that was added dropwise while shaking the tube. The suspension was left on ice for 13 min. Two original volumes of ice cold 5% sorbitol were added. The suspension was left on ice for further 10 min and then

centrifuged at 800 × g for 5 min at 4 °C. The cells were resuspended again in cold 5% sorbitol, left on ice for 8 minutes, and then centrifuged as above. The supernatant was removed and the cells were washed twice with cold RPMI 1640 complete medium. The final pellet was resuspended in RPMI 1640 complete medium again and RBCs were added to make a 2.5% haematocrit. Once the parasites have appeared in the culture and grown above 1% parasitaemia, the haematocrit was raised to usual 5%.

2.6. Synchronisation of the parasite culture

Parasites can be synchronised at a ring stage. To be more precise, other stages than rings are killed off. The cells from the culture were centrifuged at 800 × g for 5 min at RT. The cells (pellet) were resuspended in five pellet volumes of pre-warmed (37 °C) 5% sorbitol and left to incubate at 37 °C for 5 min. The suspension was centrifuged as above, all sorbitol was removed, and the resulting pellet was resuspended in RPMI 1640 complete medium.

2.7. Saponin lysis

Saponin lysis enables extraction of parasite cells from RBCs. One tenth of culture volume of, in most cases, 2% saponin (in PBS) was added to the culture. The cell suspension was left on ice for 10 min. The parasite cells were then collected by centrifugation at 2,500 × g for 10 min at 4 °C. The cells were washed two or three times until no haemoglobin traces were visible and the supernatant was clear. The final pellet was then handled according to following intentions (DNA, RNA, protein, or GSH extraction).

2.8. RNA extraction

RNA was extracted from synchronised culture at middle trophozoite stage (~ 30 h post invasion). The parasite cells were obtained by saponin lysis. The pellet (parasite cells) was resuspended in 10 pellet volumes of Trizol. RNA was extracted by addition of 1/5 of Trizol volume of chloroform. The solution was vortexed and centrifuged at 13,000 × g for 15 min at 4 °C. A clear phase resolution was created and the aqueous phase was transferred into a fresh tube. RNA was precipitated from the aqueous phase by adding 500 µl of isopropanol per initial Trizol volume of 1 ml. It was incubated at RT for 10 min. The RNA pellet was obtained by centrifugation at 13 000 × g for 15 min at 4 °C. The RNA pellet was washed in 500 µl 75% ethanol (diluted with DEPC-treated water) and immediately centrifuged as

above. The RNA pellet was air-dried for 10–15 min and then dissolved in DEPC-treated water.

2.9. Protein extraction

Proteins were extracted from a mixed culture of parasites. The parasite cells were obtained by saponin lysis. The pellet (parasite cells) was resuspended in one pellet volume of the Lysis Buffer. The cells were disrupted by three rounds of freeze (dry ice) and thaw cycles and centrifuged at 13 000 × g for 10 min at 4 °C. The supernatant was transferred into a fresh tube and the protein concentration was determined using the Bradford assay according to the manufacturer's recommendation with BSA as a standard (BioRad).

2.10. Polymerase chain reaction

Polymerase chain reaction (PCR) was carried out in a standard fashion. However, PCRs run on a *Plasmodium* spp. DNA need to have set lower extension temperature (60–68 °C) due to high A-T content.

2.11. Reverse transcription

The RNA was first treated with the Turbo DNA-free kit (Albion) to remove traces of genomic DNA at 37 °C for 30 min as recommended by the manufacturer. Then, the RNA was reverse transcribed to generate complementary DNA (cDNA) from 2 µg of total RNA with the Retro-RT kit (Albion). The reverse transcription was carried out at 42 °C for 1 hour and the reverse transcriptase was inactivated by heating at 92 °C for 10 min.

2.12. SDS-polyacrylamide gel electrophoreses and Western blot

The SDS-polyacrylamide gel electrophoreses (PAGE) were run in polyacrylamide gels with a 5% polyacrylamide stacking gel and a 12.5% and 15% separating gel at 25 mA in the presence of the Electrophoretic Buffer.

Proteins were transferred from the gel to 0.45 µm nitrocellulose membrane (Schleicher & Schuell) in a Trans-Blot SD Semi-Dry Transfer Cell (BioRad). Filter papers, the nitrocellulose membrane, and the gel were pre-soaked in the Towbin Buffer. A sandwich was then built from the pre-soaked items. The protein transfer was run at a constant voltage of 20 V and 5 Watts for one hour. Subsequently, the membrane was rinsed in PBS before it was stained with Ponceau S. The membrane was blocked overnight in 3% BSA (dissolved in

PBST) at 4 °C before it was incubated with primary antibody diluted in 1% BSA for 1 hour at RT. Before applying the secondary antibody the membrane was washed 3 times for 10 min in PBST. The secondary antibody was diluted in PBST and incubated for 1 hour at RT. To detect the presence of antigen-antibody complex, Immobilon Western Chemiluminiscent HRP Substrate (Millipore) was applied to the membrane so it was evenly covered which was then incubated for 90 sec. The membrane was drained of excessive substrate and wrapped in cling film. The signal of the HRP-conjugated antibodies was exposed to X-ray films. The membrane was stripped, if needed, in restore buffer (Fisher) as recommended and then blocked again as above. The resulting protein bands were then analysed by a densitometric software analysis (1-D Labimage, Kapelan). Even protein loading was verified by detection of a protein of a constant abundance in all parasite lines under investigation. Here antibodies detecting two proteins were chosen as loading controls: first the E2 subunit of branched chain α-keto acid dehydrogenase complex (BCKDH E2, 50 kDa) and second 2-Cys peroxiredoxin (22 kDa).

2.13. Quantitative Real-Time PCR

The Real-Time PCR reactions were set up according to the Applied Biosystem 7500 manual. In short, the primers were diluted to 3 µM concentration so that the final concentration was 300 nM. A master mix was prepared in the following way for all reactions:

1 reaction: 12.5 µl Quantitect SYBR Green
2.5 µl forward primer
2.5 µl reverse primer

At the end, 7.5 µl of a cDNA template was added into each reaction. DNA was serially diluted in this way: 80, 40, 20, 10, 5 ng/well, and NTC. In NTC wells 7.5 µl of water was added instead. The reactions were pipetted in duplicates in 96-well plate, mixed, sealed tightly, and briefly centrifuged. The thermal cycler (Applied Biosystems 7500 Real-Time PCR System) was set up:

1. 50 °C 2 min
2. 95 °C 15 min
3. 95 °C 40 repetitions 5 sec
   54 °C 30 sec
   68 °C 35 sec

The transcripts examined were amplified from the following sets of primers:

glutamate dehydrogenase b

5’-GCGTATGCAAAGAGAAGAGGAA-3

5’-GTAGAAGTATAGCCGTAGTTGTGTA-3’

glutamate dehydrogenase c

5’-TCATCGTCTCCATCATCAGTTC-3’

5’-CTCACATTACTCTGAGCACATCT-3’

glucose-6-phosphate dehydrogenase-6-phosphogluconolactonase

5’-GACCTGAATGATTTTAATTGGAAAGCA-3’

5’-CATCTATCGGAGTTCGACCTC-3’

γ-glutamylcysteine synthetase

5’- TCCTTGCTCTTACTGCATGTACT-3’

5’- TTCCGTTCTACAATCAACACTGT-3’

glutathione synthetase

5’- CTTTAGAGCATTATATACACCTAACCA-3’

5’-CGAACCAACAAGTTGATAAGGTA-3’

seryl t-RNA synthetase (Salanti et al., 2003)

5’-AAGTAGCAGGTCATCGTGGTT-3’

5’- TTCGGCACATTCTTCCATAA-3’

Dissociation curves for each primer pair were generated to verify the primer pair specificities (not shown). The efficiency of each primer in the PCR was shown by plotting cycle threshold (Ct) values against the initial D10 cDNA amounts (Fig. 5). Ct values indicate the number of PCR cycles required for the fluorescent signal to cross the threshold. The resulting equation for each primer pair was then taken into account when comparing the amount of reverse-transcribed transcripts between the cell lines. The slope (a) and y-intercept (b) of each linear equation were further used to determine relative transcript abundance (Fig. 6).

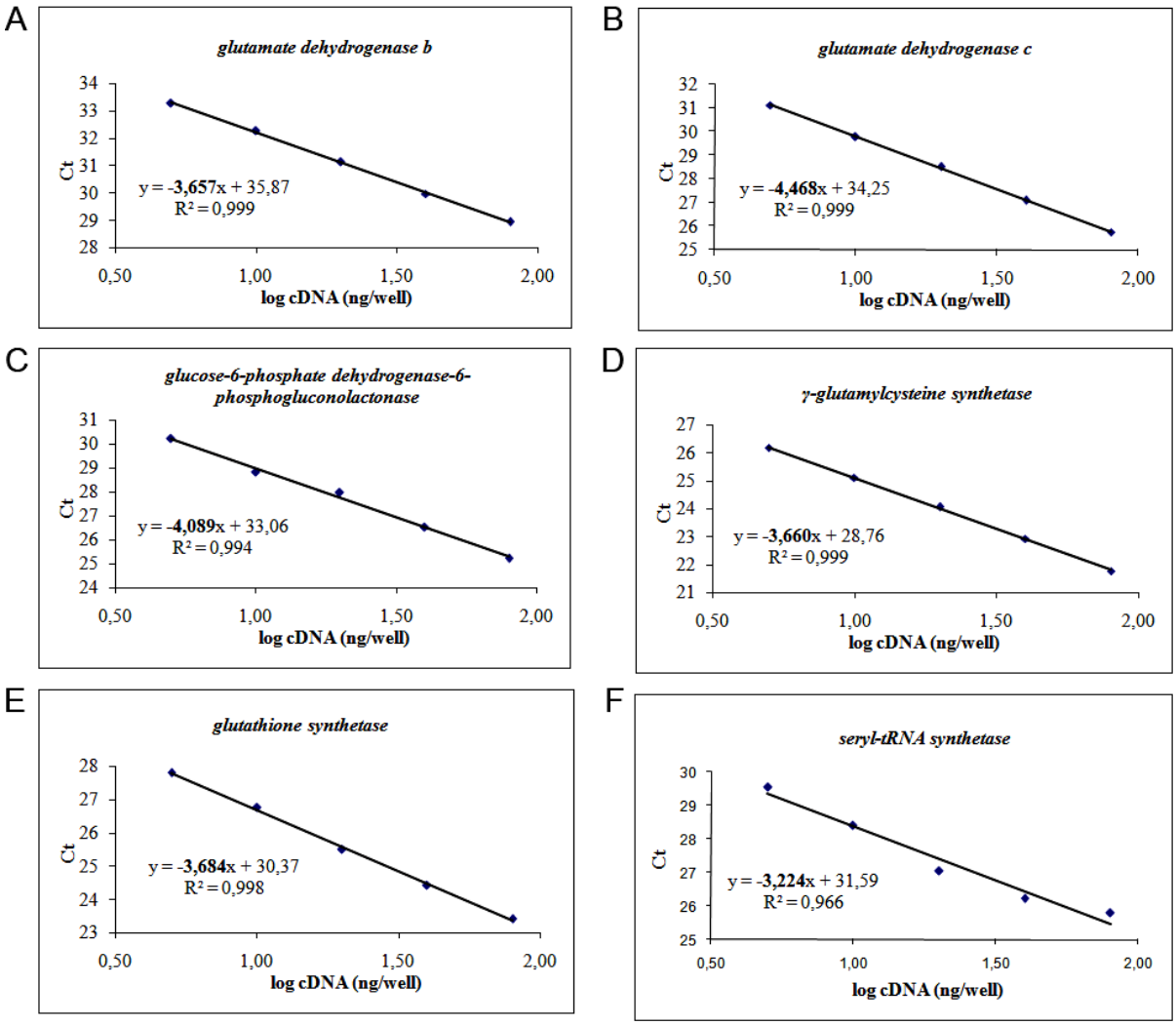

Figure 5. Primer pair efficiency curves. The slope (in bold) of the line determines the reaction doubling efficiency. Slope of around -3.3 equals 100% efficiency, i.e. doubling DNA content in each PCR cycle. A) *glutamate dehydrogenase b*, B) *glutamate dehydrogenase c*, C) *glucose-6-phosphate dehydrogenase-6-phosphogluconolactonase*, D) *γ-glutamylcysteine synthetase*, E) *glutathione synthetase*, F) *seryl t-RNA synthetase*.

$$\text{Relative transcript abundance} = \frac{10^{\wedge}\frac{Ct_{KO} - b_{KO}}{a_{KO}}}{10^{\wedge}\frac{Ct_{WT} - b_{wt}}{a_{wt}}}$$

$$\text{Normalised relative transcript abundance} = \frac{\textit{relative transcript abundance} \text{ of gene of interest}}{\textit{relative transcript abundance} \text{ of endogenous control}}$$

Figure 6. Formula for normalised relative transcript abundance calculation. Relative transcript abundance compares unlogged transcript levels between knockout and wild type parasites. Normalised relative transcript abundance takes an endogenous control into account.

Next, 20 ng of cDNA of different parasite lines were tested for a particular transcript abundance that were compared to primer-pair-specific standard curves. Each parasite line was analysed in duplicate and one NTC per primer pair. The reactions were set up and run as above. Normalised relative transcript abundances were then calculated.

2.14. Glutathione extraction

Glutathione was extracted from 25 ml parasite culture at 2 to 4% parasitaemia. It was critical to harvest the parasites at early trophozoite stage (14 h after synchronisation) because the levels of glutathione change considerably at different developmental stages of the parasites. The parasite culture was synchronised twice with a 4 hour gap approximately 60 hours before the harvest. The RBCs were lysed using 0.2% saponin for 5 min on ice and centrifuged at 2,500 × g for 5 min at 4 °C with slow deceleration. The supernatant was removed and 1 µl of cells was taken to inspect the state of cells under a light microscope. Healthy early trophozoites have a typical haemozoin particles moving around in their food vacuole. The remaining cells were carefully resuspended in 1 ml EBSS and transferred into an ambra coloured tube. The cells were centrifuged at 2,500 × g for 3 min at 4 °C. The cells were washed in a same fashion two more times with EBSS. Before the last centrifugation, once the pellet was resuspended, 10 µl of the suspension was taken and diluted in 190 µl of EBSS to determine the parasite number in a haemocytometer. The rest of the cells was centrifuged as above, the resulting pellet was resuspended in 50 µl of Reducing Buffer, and incubated at room temperature for 45 min to allow the reduction of thiols. The glutathione standards were treated in the same way in Reducing Buffer. After 45 minutes 50 µl of monobromobimane was added into the samples and standards. Monobromobimane stays non-fluorescent until conjugated and specifically binds to low molecular thiols. The samples and standards were incubated at 70 °C for 3 min. The derivatisation was stopped by adding 4 M methanesulphonic acid pH 1.6 and incubating for 30 min on ice to precipitate proteins in the sample. The samples and standards were then centrifuged at 14,000 × g for 7 min at 4 °C. The supernatants were transferred in fresh tubes and centrifuged as above for further 40 min to remove the denatured proteins. 200 µl of the supernatants was then transferred into high-pressure liquid chromatography (HPLC) vials.

2.15. HPLC

HPLC was done on an UltiMate HPLC system (Dionex) and a GEMINI C18 column (Phenomenex). The mobile phase consisted of two solvents: solvent A, 0.25% acetic acid, and solvent B, 100% acetonitrile. Metabolites were separated at a flow rate of 0.55 ml/min by application of the following gradient (% of solvent B): 0 min: 0%; 10 min: 0%; 40 min: 8%; 100 min: 15%; 110 min: 50%; 111 min: 0%; 121 min: 0%. Thiols were detected using a fluorescence detector (excitation, 365 nm; emission, 480 nm). Glutathione was identified by the same retention time with its standards. The resulting peak areas were compared with standard peak areas to determine nmols of glutathione/10^{10} cells (Williams et al., 2009).

2.16. $NADP^+$ and NADPH extraction

Parasites were extracted from 25 ml culture at 5% parasitaemia per assay. The parasites were extracted, washed, and counted as described above for the glutathione extraction. The final pellet was resuspended in 400 µl of ice cold extraction buffer that was provided with the NADP/NADPH Quantitation Kit *(*Promokine) or the Extraction Buffer that was adopted and adjusted according to Zerez et al. (1988). The parasites were then subjected to three freeze-and-thaw cycles. The samples were centrifuged at 13,000 × g for 5 min at 4 °C. The supernatant was centrifuged and concentrated using 10-kDa cut-off centrifugal filters units (Millipore) at 13,000 × g for 10 min at 4 °C to remove NADPH- or $NADP^+$-consuming enzymes. The total NADP(H) pool (NADPt) was then determined in the flow-through and compared to standard curves. Unlike $NADP^+$, NADPH exhibits absorption at 340 nm with the molar extinction coefficient at this wavelength of 6.22 $mM^{-1}cm^{-1}$. It was assessed whether the standard NADPH provided was fully reduced by verifying that the absorbance of 100 µM NADPH solution at 340 nm was close to 0.622. Afterwards the standard curve was generated.

2.17. $NADP^+$ and NADPH detection by cycling reaction

NADPH samples were heated to 60 °C for 30 min to remove thermo-sensitive $NADP^+$ from the solution. The samples were then cooled on ice and centrifuged at 13,000 × g for 1 min at 4 °C. NADPt samples were not heated and were kept on ice during NADPH samples heating. Each sample and standard was diluted as shown below to make up a 50 µl sample volume. 10-µl samples were also spiked with 20 pmol of NADPH and $NADP^+$, respectively:

Sample	Extraction buffer
10 µl	40 µl
20 µl	30 µl
30 µl	20 µl
40 µl	10 µl
10 µl + 20 pmol NADPH	38 µl
10 µl + 20 pmol $NADP^+$	38 µl

The kit containing $NADP^+$ cycling enzyme mix and enzymatic buffer (100 µl) were then added to the samples and incubated for 5 min at RT. NADPH developer (10 µl) was then added and incubated for 1–4 hours. The absorbance was read at 450 nm.

2.18. The half maximal inhibitory concentration (IC_{50})

The inhibition of incorporation of [8-^{3}H]hypoxanthine by parasites into their nucleic acids is indicative of an inhibitory activity of a drug as the parasite purine metabolism relies solely on the purine(-derived) salvage. The IC_{50} value was determined on a synchronised culture at ring stage of 0.5% parasitaemia at 2% haematocrit. Every drug was dissolved in IC_{50} medium, serially diluted, and tested in duplicate for each parasite line in a 96-well plate. After the drug was added, the parasites were incubated for 48 h at 37 °C. After the incubation, half of the medium was removed and fresh IC_{50} medium with [8-^{3}H]hypoxanthine (0.4 µCi per well) was added. The culture was incubated for 24 hours at 37 °C. After the incubation, the cultures were frozen to kill the parasites. Once thawed out, the parasites were harvested on a filter mat (Wallac Printed Filter Mat A) in a Tomtec Mach III cell harvester. The radioactive signal was detected in the presence of beta scintillation fluid in a Wallac Trilux MicroBeta counter.

2.19. Transfection of *P. falciparum* and gene knockout

The construct for *glutamate dehydrogenase b (gdhb)* knockout was generated by a technician Fiona McMonagle using restricting and cloning methods. The pCC-4 construct (Fig. 7) was used to generate a knockout cell line. Parasites were transfected at a ring stage and the culture was of 8–10% parasitaemia, 5% haematocrit. The culture was centrifuged and the pelleted cells were washed in Cytomix. DNA (100 µg dissolved in 10 mM Tris-HCl, pH 7.6) prepared for the transfection was dissolved in Cytomix, mixed, and then added to

the cells. This suspension was transferred to a 2-mm electroporation cuvette. The DNA was introduced in the cells at voltage of 310 V and capacitance of 950 µF using Gene Pulser II System (BioRad). The transfected suspension was transferred into a new flask with fresh blood and medium. This culture was gassed and incubated at 37 °C for 6 hours before the medium was changed and 20 µg of blasticidin-S was added per 10 ml culture to select for the transformants that contained blasticidin-S deaminase carrying plasmid. The plasmid also carried the cytosine deaminase (CD), which allows negative selection of the parasites that still contained the plasmid, i.e. this selection was applied to remove parasites that retained the plasmid where yet no integration had taken place. CD metabolizes cytosine to uracil and this enzyme is absent from eukaryotic cells and on the plasmid enables deamination of innocuous compound 5-fluorocytosine to the highly toxic 5-fluorouracil.

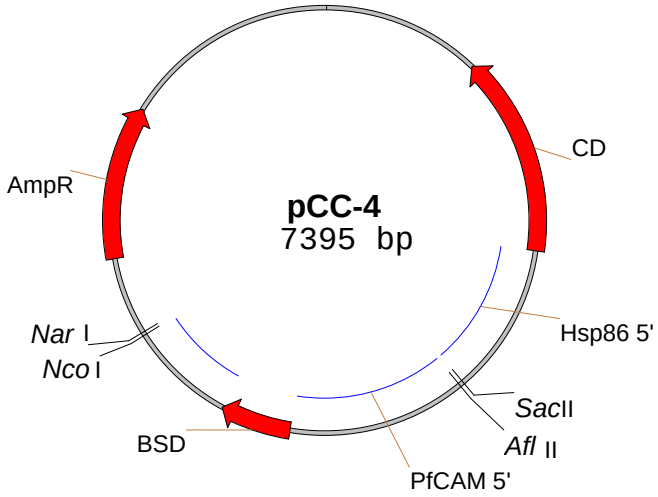

Figure 7. pCC-4 transfection construct. The pCC-4 transfection construct generates double knockouts of *P. falciparum*. The construct bears two cloning sites for 3´ and 5´- end recombination of the gene of interest. First cloning site can be cut by Nar I and Nco I restriction enzymes and the second cloning site can be cut by Sac II and Afl II. Furthermore, the plasmid contains ampicillin resistance cassette (AmpR) for selection in bacterial culture. Apart from that, the construct contains two genes for both positive and negative selection in the parasite. Blasticidin-S deaminase gene (BSD) is controlled by a calmodulin promoter (PfCAM 5´). Cytosine deaminase (CD) gene is controlled by heat shock protein 86 promoter (Hsp86 5´).

2.20. Statistics

Statistical analyses were conducted in GraphPad Prism software. The analysis for all data tested was done by one-way analysis of variance (ANOVA) followed by Turkey´s multiple comparison test.

3. Results

3.1. *Glutamate dehydrogenase a* knockout confirmation by Western blot

Glutamate dehydrogenase a knockout (Δ*gdha*) of *Plasmodium falciparum* was generated and the gene disruption was confirmed by Southern blot analysis by Dr. Janet Storm (not shown). Two mutant cell lines (clone 1 and clone 2) were maintained in culture for further analyses. These mutant cell lines were subjected to Western blot analyses to verify total depletion of the GDHa protein. GDHa (50 kDa) was detected only in the wild type cell line, D10. No protein was detected in mutant parasite lines. The protein (~34 kDa) that was also detected non-specifically by the GDHa antiserum served as a loading control (Fig. 8).

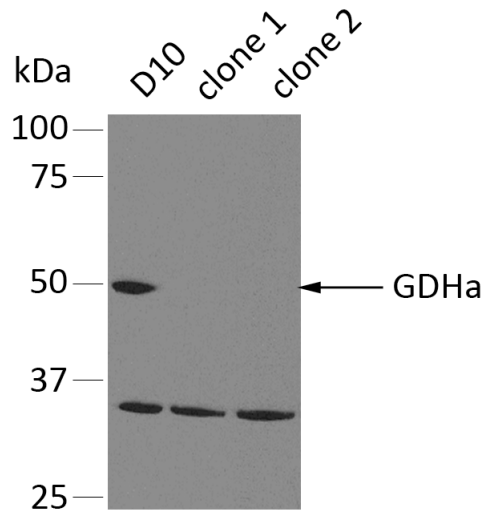

Figure 8. Deletion of glutamate dehydrogenase a (GDHa). The Western analysis shows that the GDHa protein (1:2000; 50 kDa) is no longer present in the mutant parasite clones 1 and 2. GDHa was detected using a polyclonal antiserum in wild type D10 parasites. A second protein (34 kDa) was also detected by the antiserum which is present in all three lanes of the blot.

3.2. Viable knockout parasites regardless of oxygen tension

To examine whether the mutant parasite lines have any growth defects or if they are more susceptible to elevated oxygen tension, they were incubated in an atmosphere of 1% or 20% oxygen, respectively. Thin blood smears from three independent cultures were generated daily and the parasitaemia in 1000 red blood cells was determined per thin smear. Every second day, the parasite cultures were diluted five times. It was shown that Δ*gdha* null mutants did not display any growth defect during the intraerythrocytic development under normal culturing conditions at 1% oxygen. Moreover, mutant cell lines displayed the same growth and replicating pattern as the wild type even under elevated oxygen tension at 20% oxygen (Fig. 9).

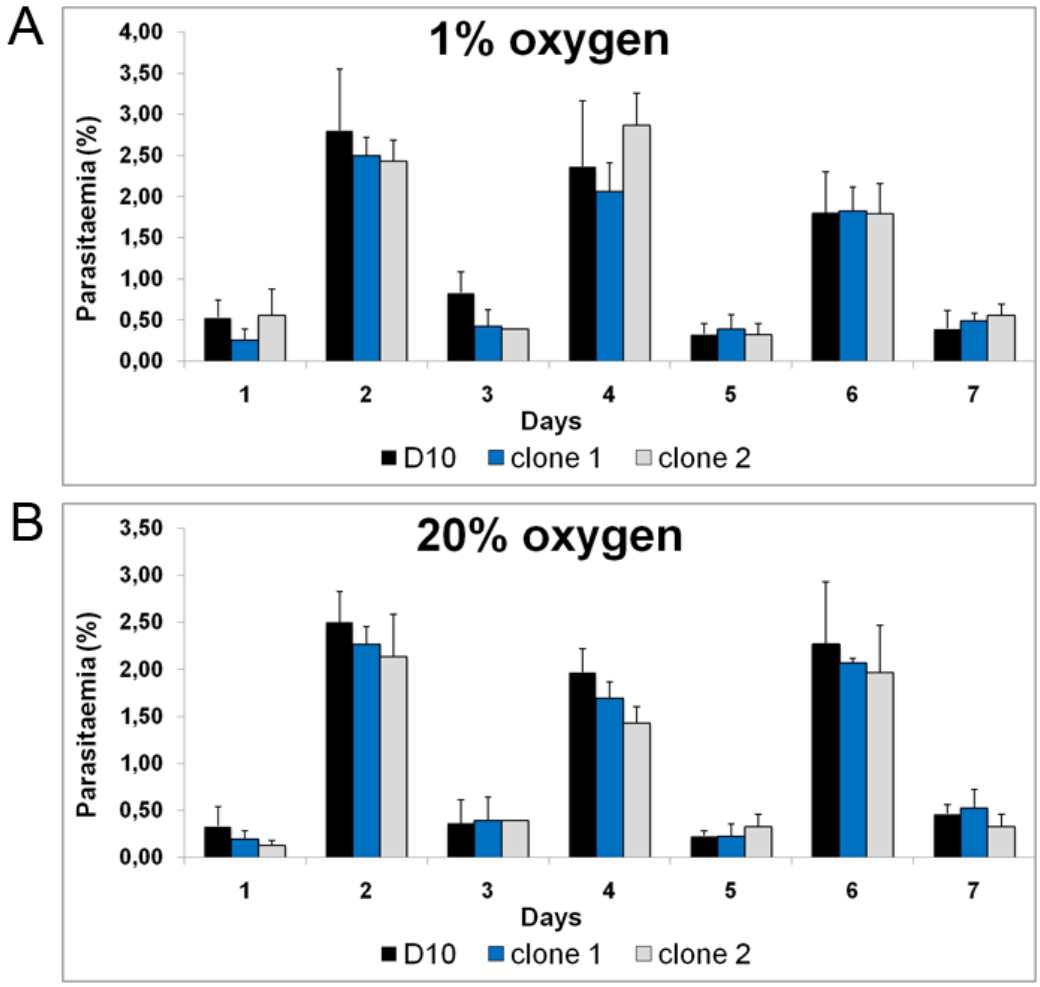

Figure 9. Growth of wild type D10 and Δ*gdha* clones 1 and 2 over seven days. The growth curve shows that wild type and Δ*gdha* mutant parasite lines have an equal growth rate regardless of the oxygen tension they encounter. Each value was derived from three independent Giemsa-stained thin blood smears and parasitaemia per 1000 erythrocytes was determined. Every cell line was diluted five times every second day. One positive standard deviation is indicated. Wild type (D10) and mutant cells (clone 1, clone 2) were observed for seven days A) under 1% oxygen tension and B) under 20% oxygen tension.

3.3. Comaparable sensitivities to stress-inducing molecules

It was hypothesized that the major role of GDHa in *P. falciparum* is to provide the cell with the reducing molecule NADPH. NADPH is used as a cofactor for important reducing reactions in redox and antioxidant systems. We suspected that cutting off the source of NADPH may thus lead to the parasite experiencing redox or antioxidant discomfort. In that view, the parasite susceptibility to oxidative stress was further assessed by exposing the mutant cell lines to stress-inducing pro-oxidant molecules. Drugs were serially diluted and incorporation of [8-^{3}H]hypoxanthine was indicative of cells viability. The half inhibitory values were determined for *tert*-butyl hydroperoxide (exogenous stressor, t-BuOOH) and N-methylphenazonium methosulphate (endogenous stressor, PMS). t-BuOOH and PMS alike

showed no differential effect on the viability of wild type and mutant parasites (Fig. 10, Fig. 11). These results are very surprising as it was hypothesized that the production of NADPH by GDHa should have a direct input into antioxidant defence. These data, though, do not support this hypothesis.

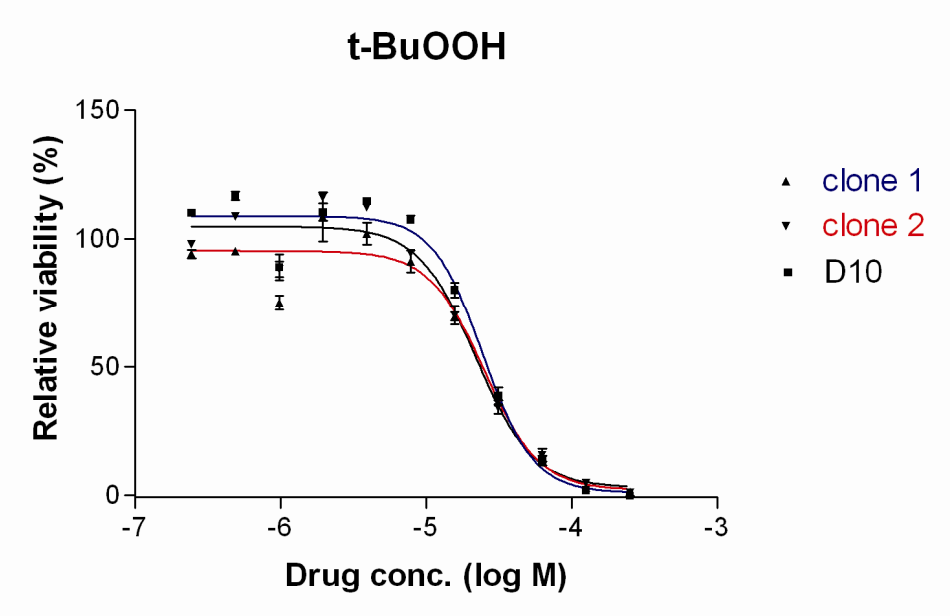

Cell line	IC_{50} value (µM ± 1 S.D.)
D10	39.5 ± 25.0
clone 1	46.4 ± 31.0
clone 2	43.4 ± 26.2

Figure 10. t-BuOOH impaired viability of mutant lines similarly to wild type cells. The graph plots the relative viability of the mutant (clone 1, clone 2) and wild type (D10) cells in the presence of serially diluted t-BuOOH, ranging from 240 nM to 250 µM, as a sigmoidal dose-response curve. Each point on the graph represents an average of two measurements plus their standard deviations. The half maximal inhibitory concentration (IC_{50}), i.e. the concentration of a drug that is required for 50% inhibition *in vitro*, was then obtained from the graph. The average IC_{50} values of four datasets and their standard deviations (S.D.) are shown in the table under the graph together.

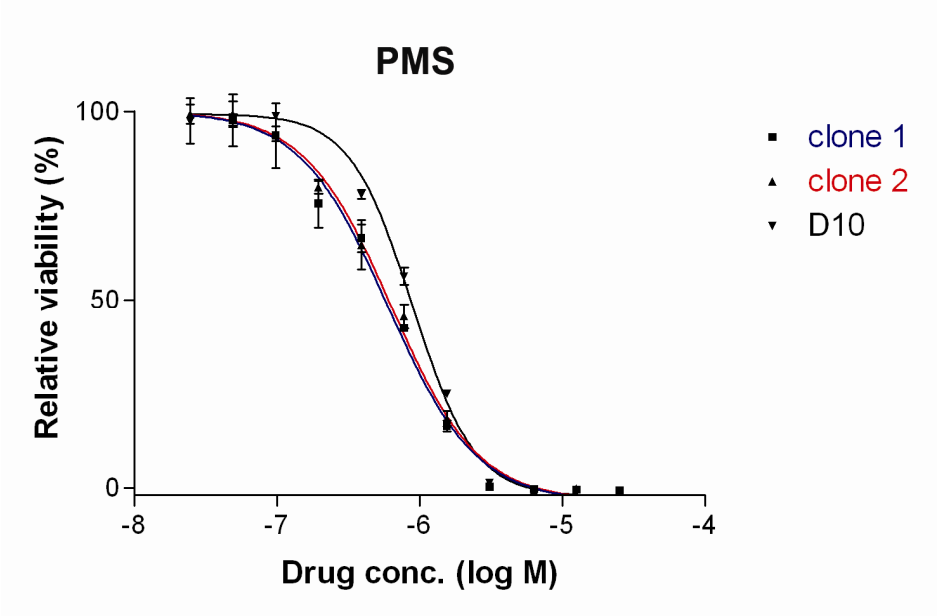

Cell line	IC_{50} value (µM ± 1 S.D.)
D10	0.76 ± 0.18
clone 1	0.74 ± 0.20
clone 2	0.69 ± 0.09

Figure 11. Viability of parasites in the presence of endogenous stressor PMS. The graph compares the drug sensitivity of mutant (clone1, clone 2) and wild type parasites (D10). The values on the graph represent the relative viability of the cells in the presence of serially diluted drug, ranging from 24 nM to 25 µM, plus their respective standard deviations (S.D.) from 2 independent measurements. The average IC_{50} values of four datasets and their standard deviations (S.D.) are shown in the table underneath.

3.4. NADPH and $NADP^+$ quantification

The obvious solution to assess the role of GDHa in providing NADPH for the cell, and thus being an important link in a redox system of *P. falciparum*, is to measure NADPH and $NADP^+$ content in the mutant and wild type parasites and compare them to each other. First, it was tried to measure the content of the dinucleotides according to Promokine NADP/NADPH Quantitation Kit manual. It appeared that technical problems prevented the assay from functioning satisfactory. The major problem seemed to be the extraction step as it was not possible to measure the parasite NADP(H) content. Nevertheless, the assay was functional for measuring commercial NADPH and $NADP^+$ for which it was very sensitive. Dissolved in the extraction buffer, 20 nmol of NADPH was measured to be 16 nmol and 20 nmol of $NADP^+$ as 21 nmol. When heated at 60 ^oC, NADPH was measured as 23 nmol and no $NADP^+$ was detected. It was even easily feasible to measure as low as 20 pmol of spiked $NADP^+$ in the cell extract. These data do not support the suspicion that some cellular component would inhibit the assay. However, even with some adjustment to the extraction

step like using Extraction Buffer as in Zerez et al. (1988) or removing potential dinucleotides utilizing enzymes, the assay did not measure any parasite NADP(H) content. Since we failed to directly evidence the role of GDHa as an NADPH producer, we resorted to analyse relative antioxidant protein and RNA abundances.

3.5. Unaffected protein levels of antioxidant and redox enzymes

Superoxide dismutase

Superoxide dismutases (SOD) constitute the first line of defence against ROS. Even though the enzymes are not directly dependent on NADPH availability, it was interesting to examine if this enzymatic front line defence was affected by the absence of GDHa. This was assessed by measuring SOD protein levels by Western blotting. The band densities of SOD1 and SOD2 detected by specific SOD1 and 2 antibodies in the mutant parasites were compared to the expression levels of the two SOD proteins in D10 wild type parasites. The SOD2 antibody detected two bands around the expected size so the double band was used for the densitometric analysis. Each Western blot was done twice using independently generated protein lysates. There were no statistically significant ($p < 0.05$) differences in the SOD1 and 2 protein levels between the D10 wild type and mutant parasites (Fig. 12).

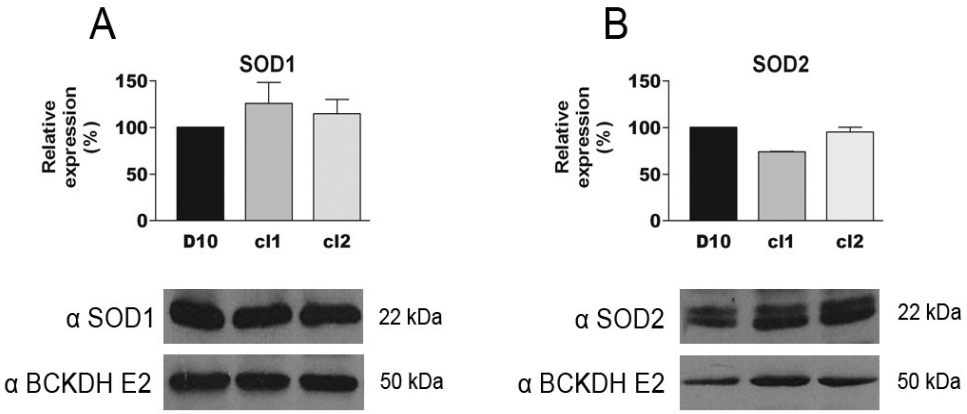

Figure 12. Abundance of Superoxide Dismutase 1 and 2. Relative expressions in mutant parasites are shown in the top graphs and the respective Western blots are shown beneath. A) Top graph shows superoxide dismutase 1 (SOD1) expression in mutant cells (cl1, cl2) relative to SOD1 expression in wild type (D10). One standard deviation is indicated. The bottom panel shows a Western blot detecting SOD1 (1:5000; 22 kDa) and a loading control E2 subunit of branched chain α-keto acid dehydrogenase complex (BCKDH E2; 1:5000; 50 kDa). B) Top graph shows superoxide dismutase 2 (SOD2) expression in mutant parasites (cl1, cl2) relative to SOD1 expression in wild type parasites (D10). One standard deviation is indicated. The bottom panel shows a Western blot detecting SOD2 (1:5000; 22 kDa) and a loading control BCKDH E2 (50 kDa).

Peroxiredoxins

Peroxiredoxins catalyse the reduction of hydrogen peroxide. As such, peroxiredoxins constitute an indispensible link with SODs to reduce hydrogen peroxide produced by SODs. The active cysteine(s) in peroxiredoxins get(s) reduced by thioredoxin which gets reduced by NADPH-dependant thioredoxin reductase. Peroxiredoxins are thus directly dependent on the supply of NADPH. Their expression levels in the absence of GDHa were assessed as above. Protein levels of peroxiredoxins showed no statistically significant difference ($p < 0.05$) in the absence of GDHa (Fig. 13).

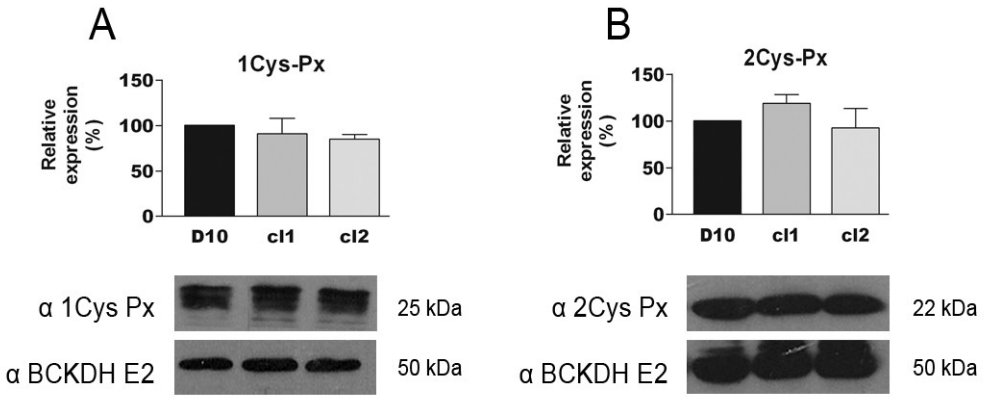

Figure 13. Abundance of 1Cys and 2Cys Peroxiredoxin. Western analysis of two parasite peroxiredoxins (Px) are shown below their relative expression graphs. A) The Western blot of 1Cys Px (1:75000; 25 kDa). B) The Western blot of 2Cys Px (1:100000; 22 kDa). The even loading is controlled in both cases by BCKDH E2.

Glutathione reductase and thioredoxin

P. falciparum possesses two functional redox systems. These are thioredoxin and glutathione redox system, respectively. To assess if GDHa absence has any impact on redox homeostasis, on protein level, thioredoxin (Trx) and glutathione reductase (GR) were tested by Western blot analyses. Thioredoxin is enzymatically reduced by NADPH-dependant thioredoxin reductase. Glutathione reductase, another NADPH-dependant oxidoreductase, regenerates glutathione that got oxidized in the repair of oxidative damage. None of the proteins tested displayed any statistically significant ($p < 0.05$) down- or up-regulations in the mutant parasite lines (Fig. 14).

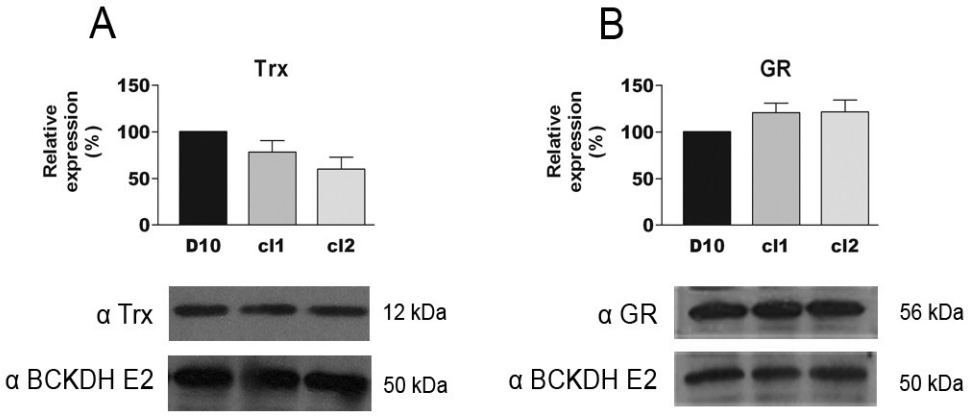

Figure 14. Abundance of Thioredoxin and Glutathione Reductase. Western analysis of parasite cytosolic thioredoxin (Trx) and glutathione reductase (GR) is shown together with relative expression graphs. A) The Western blot of Trx (1:10000; 12 kDa). B) The Western blot of GR (1:100000; 56 kDa). The even loading is controlled by BCKDH E2.

Isocitrate dehydrogenase and glutathione S-transferase

Isocitrate dehydrogenase (IsoDH) is together with GDHa an NADPH-producing enzyme in *P. falciparum*. IsoDH was also suggested as a main NADPH producer of the parasitic cell (Vander Jagt et al., 1989). The potential catalytic takeover was tested by Western blot as above (Fig. 15A). Glutathione S-transferase (GST) catalyses the ligation of glutathione to electrophiles and thus renders toxic compounds and reactive oxygen species harmless (Müller, 2004). Since glutathione needs to be in a reduced state as a GST cofactor and the reduction is catalysed only by NADPH-dependant glutathione reductase, the GST expression was hypothesized to be affected by GDHa depletion. The relative expression level of GST was tested as above (Fig. 15B). Neither IsoDH nor GST showed any statistically significant ($p < 0.05$) deviation of their protein levels in the mutant cells.

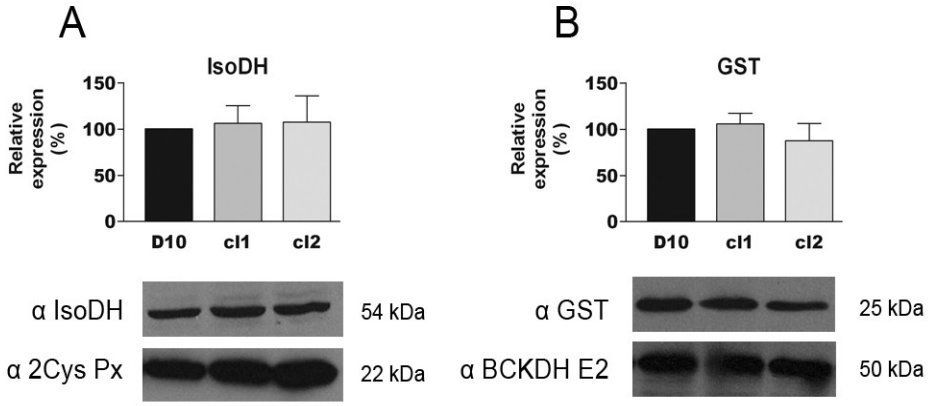

Figure 15. Abundance of Isocitrate Dehydrogenase and Glutathione S-Transferase. Western analysis of parasite mitochondrial isocitrate dehydrogenase (IsoDH) and cytosolic glutathione S-transferase (GST) together with relative expression graphs. A) The Western blot of IsoDH (1:30000; 54 kDa) and 2Cys Px as a loading control. B) The Western blot of GST (1:20000; 25 kDa) and a BCKDH E2 loading control.

3.6. Slight up-regulations of transcript levels for GSH biosynthesis and NAD(P)H-producing enzymes

In order to assess if any transcriptional levels of glutathione biosynthesis enzymes or NAD(P)H-generating enzymes was up- or down-regulated, their RNA levels were compared by quantitative Real-Time PCR. The transcript levels were detected using primers whose specificities for the transcript were verified. The genomic DNA (gDNA) PCR showed a clear specificity of every primer pair that always amplified only one visible band. This was not true only for *gdhb* amplicon as its forward primer was designed over two exons and the gDNA PCR resulted in no visible band formation. Further, the primer specificity was verified by the dissociation curve analysis by virtue of only single peaks detection. As a result, SYBR green fluorescence can be considered a direct measure of accumulation of the transcript of interest. Each sample was run on two independent total RNA extracts.

Glutamate dehydrogenase b, glutamate dehydrogenase c, and glucose-6-phosphate dehydrogenase-6-phosphogluconolactonase

Glutamate dehydrogenase b (gdhb) and *glutamate dehydrogenase c (gdhc)* encode for two other glutamate dehydrogenases, b and c (http://www.PlasmoDB.org; database version 7.1). These two enzymes were not primarily suggested as the main NADPH source for the cytosol because GDHb was speculated to be localized in the apicoplast and GDHc is supposedly NAD^+-specific (http://www.PlasmoDB.org; database version 7.1). Nevertheless, their potential involvement in supplying NADPH to the cell has not been experimentally addressed yet. Glucose-6-phosphate dehydrogenase-6-phosphogluconolactonase (G6PD6PGL), on the other hand, has been tested numerous times for its activity and its potential to provide NADPH for the cell but its genuine contribution still remains debatable. To investigate if the gene transcription of *g6pd6pgl* is activated in the absence of GDHa to meet the NADPH demand, its gene transcript abundance was tested as well. Quantitative Real-Time PCR showed no significant change in normalised relative transcript abundances that could be considered as biological important. Slight up-regulations of the transcripts tested were observed (Fig. 16).

γ-Glutamylcysteine synthetase and glutathione synthetase

γ-glutamylcysteine synthetase (*γgcs*) and *glutathione synthetase* (*gs*) code for the two biosynthetic enzymes of glutathione. We speculated that these two enzymes may be up-regulated in the absence of GDHa to sustain the constant GSH/GSSG ratio as GR activity

may be potentially affected by an imbalance of the $NADP^+$/NADPH ratio as a consequence of the *gdha* gene deletion. Moreover, in the absence of GDHa, the parasite may accumulate glutamate, one of the amino acids required for GSH biosynthesis which may influence the γ-glutamylcysteine production. It was shown, though, that these gene transcripts also exhibit only slight increases in their normalised relative transcript abundances (Fig. 16).

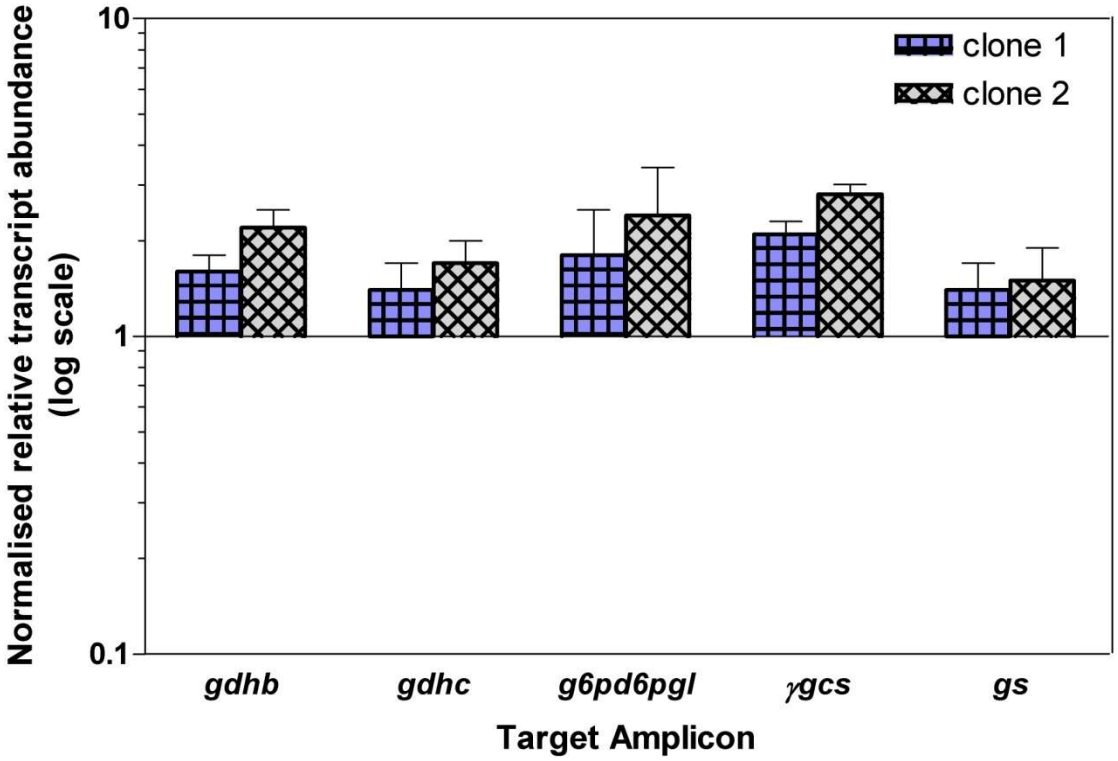

Figure 16. Fold change of the particular transcript concentration of Δ*gdha* parasites (clone 1 and 2) relative to D10 and normalised to *seryl-tRNA synthetase* transcript concentration. The gene transcripts examined: *glutamate dehydrogenase b* (*gdhb*), *glutamate dehydrogenase c* (*gdhc*), *glucose-6-phosphate dehydrogenase-6-phosphogluconolactonase* (*g6pd6pgl*), *γ-glutamylcysteine synthetase* (*γgcs*), and *glutathione synthetase* (*gs*). The reached values signify an average of two independent experiments run in duplicates plus their respective 1 S.D.

3.7. Increased glutathione pool levels

In order to verify if the ~2 fold higher levels of the *γgcs* transcript lead to an actual increase in glutathione levels, total glutathione from the mutant parasites was quantified by high-pressure liquid chromatography (HPLC) and compared to the GSH level in wild type parasites. The glutathione pool was extracted from the freed parasites, the oxidised glutathione molecules reduced using TCEP, and then the reduced GSH molecules were derivatised using monobromobimane. All cellular thiols were separated by reversed-phase liquid chromatography. My data show that the GSH levels increased from 486 nmoles/10^{10}

parasites in D10 parasites to 1866 and 1421 nmoles/10^{10} Δ*gdha* mutant parasites suggesting that the mutants contain elevated GSH levels. This was repeated only once and in the second experiment, the data were 391 nmols/10^{10} parasites in D10 parasites compared to 1210 and 908 nmoles/10^{10} parasites in the clone 1 and 2, respectively (Fig. 17).

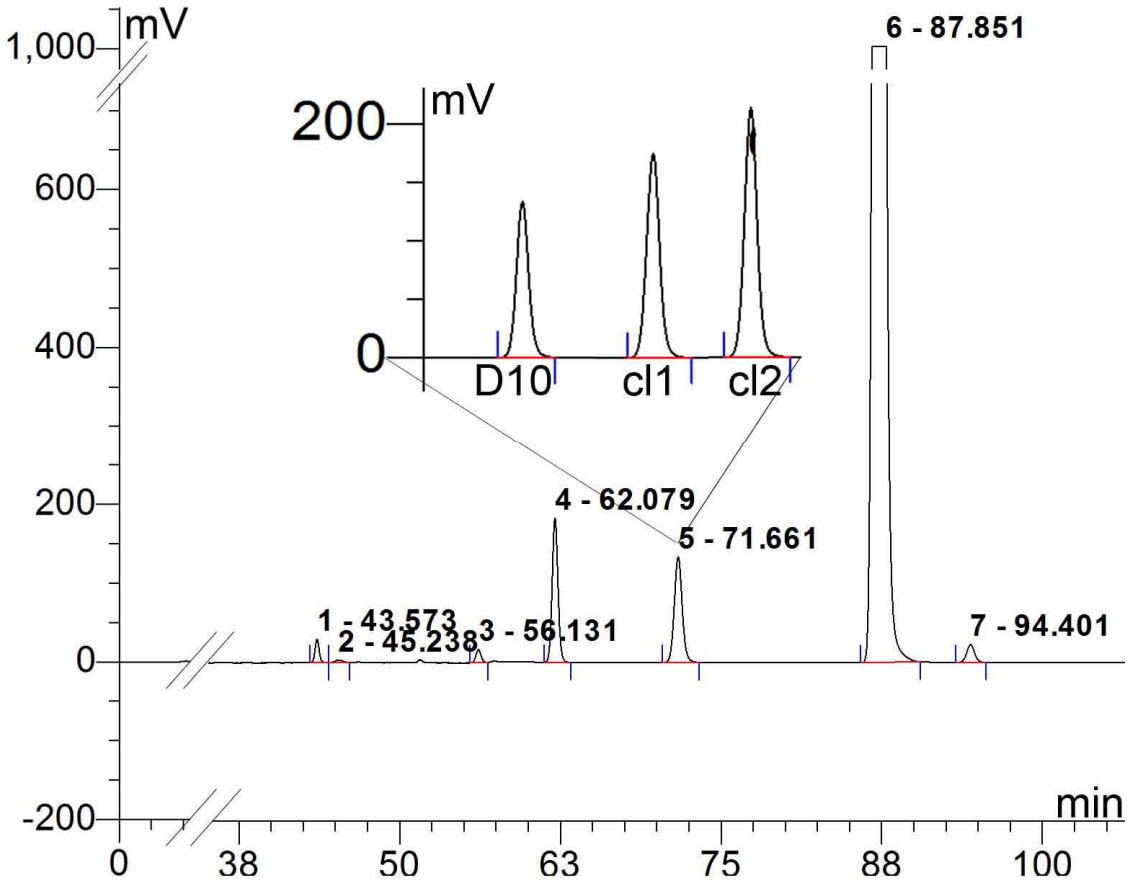

Cell line	GSH concentration (nmol/10^10 cells) ± 1 S.D.
D10	438,51 ± 67,85
clone 1	1537,66 ± 464,06
clone 2	1164,36 ± 362,96

Figure 17. Elution profile of monobromobimane derivatised thiols of D10 parasites. The elution profile was obtained from freed parasites from 25 ml culture. Thiol-containing molecules were detected by their retention times (min) in comparison with standards. Glutathione is eluted at 71 min. The peak at 43 min represents cysteine. The peak at 62 min as well as the peak at 87 min represents a solvent. The glutathione peaks from D10 and Δ*gdha* mutant parasites are compared in the inset. Glutathione average amounts per 10^{10} cells from two independent extractions are shown in the table below.

3.8. Aminotransferase selective inhibition

P. falciparum GDHa was suggested to favour the oxidation reaction in which glutamate is converted into 2-oxoglutarate and NADPH is generated (Wagner et al., 1998). Apart from GDHa, the conversion of glutamate to 2-oxoglutarate is also catalysed by aminotransferases, three of which are also encoded for in *P. falciparum* genome. The susceptibility of the parasites to L-cycloserine, an aminotransferase inhibitor, was tested. This analysis revealed a statistically significantly ($p < 0.01$) different susceptibility to this drug suggesting that Δ*gdha* mutant parasites are more susceptible to the aminotransferase inhibitor than the wild type parasites (Fig. 18). These data imply that the Δ*gdha* mutants rely more on the activity of aminotransferase than wild type parasites.

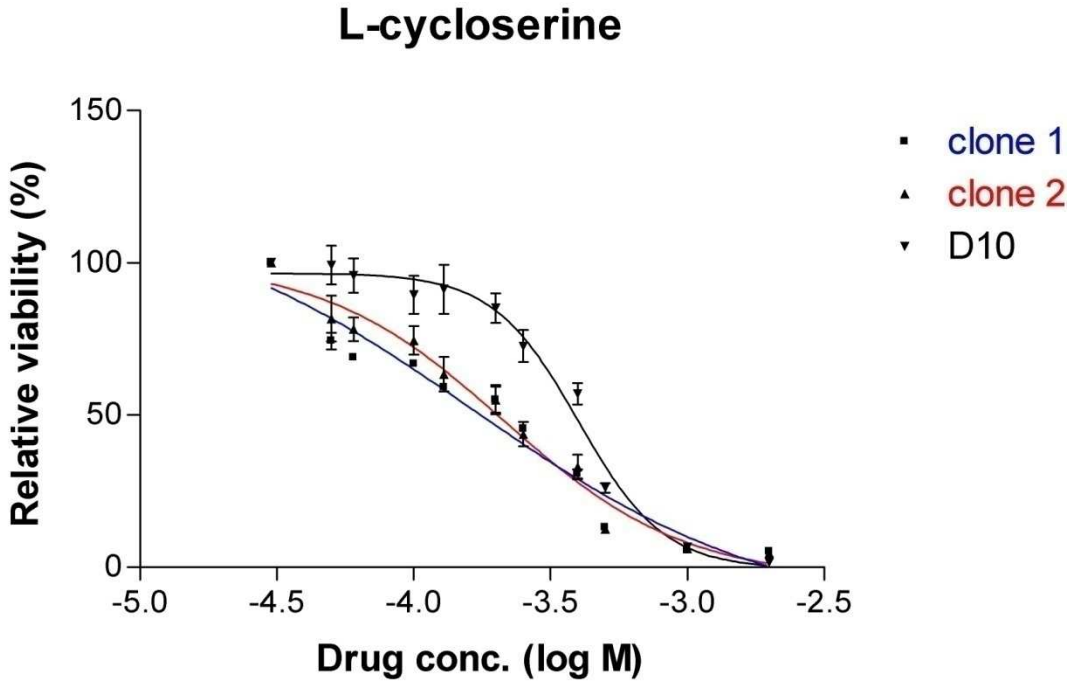

Cell line	IC_{50} value (µM ± 1 S.D.)
D10	272.0 ± 1.5
clone 1	151.0 ± 6.7*
clone 2	171.6 ± 21.3*

Figure 18. Susceptibility of D10 wild type and Δ*gdha* mutant parasites to L-cycloserine. Viability of the cells is plotted on a graph in dependence on increasing drug concentration, ranging from 30 µM to 2 mM. Each point represents a relative viability of the cells from two measurements ± standard deviation (S.D.). IC_{50} values from four datasets together with their standard deviations (S.D.) are put in the table below. * denotes a statistically significant difference in IC_{50} values ($p < 0.01$). Statistical analyses were performed with ANOVA followed by Turkey´s multiple comparison test.

3.9. *Glutamate dehydrogenase b* knockout construct transfection

To elucidate the role of glutamate dehydrogenase b (GDHb), another potentially NADPH-producing enzyme, D10 cell line was transfected with a knockout construct, pCC4 (Fig. 7). As the intraerythrocytic stages of the parasite contain a halpoid genome, only one locus had to be disrupted. The transfected cell line was cultured in the presence/absence of selectable markers for several months. This procedure should promote integration of the construct into the parasite´s genome. Even after three rounds of on and off drug cycling, no integration was achieved. This was evidenced by a PCR of gDNA isolated from transfected parasites (Fig. 19).

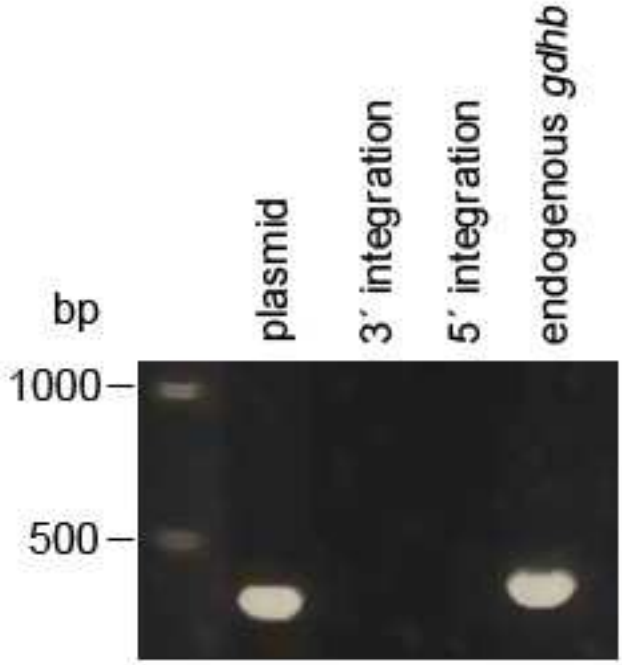

Figure 19. No integration of either part of the knockout construct in the transfected cells. In lane 1, the transfecting plasmid was detected. Lane 2 and 3 show no 3´ or 5´ integration. In lane 4, endogenous *gdhb* was detected.

4. Discussion

Redox homeostasis constitutes a vital mechanism for the malaria parasite *Plasmodium falciparum* during its intraerythrocytic development as it is exposed to high oxidative challenges (Turrens, 2004). The redox systems have been intensely studied yet some fundamental questions remain unanswered. NADPH is a dinucleotide cofactor that is required for some oxidoreductases that maintain the redox balance of the cell. To date, no enzyme with dominant NADPH producing activity has been described in the parasite (Roth et al., 1986; Yoshida and Roth, 1987; Vander Jagt et al., 1989). Glutamate dehydrogenase a (GDHa) has been suggested as a potential candidate for NADPH production in *P. falciparum*. The parasite encodes three glutamate dehydrogenases two of which appear to be NADP(H) specific, GDHa and GDHb. GDHa is a cytosolic enzyme and has been experimentally shown to display $NADP^+$ specificity (Wagner et al., 1998). Mammalian GDH, that is NAD(P)H specific, is not present in human red blood cells (Vander Jagt et al., 1982). Given these facts, GDHa represents a good malaria marker and a possible drug target (Wagner et al., 1998; Werner et al., 2005; Aparicio et al., 2010).

Similar oxidative stress susceptibility

Disruption of the *gdha* locus has no effect on the intraerythrocytic development of *P. falciparum*. More surprisingly, the parasite is indifferent to oxidative stresses like elevated oxygen tension, *tert*-butyl hydroperoxide (t-BuOOH), or N-methylphenazonium methosulphate (PMS) action. Culturing the parasite at elevated oxygen tension for the course of seven days constitutes a highly oxidative environment for the parasites which are usually maintained at 1% oxygen tension in the *in vitro* culture system. The establishment of continuous cultures of *P. falciparum* dates back to 1976 when Trager and Jensen (1976) devised an *in vitro* culturing system for *P. falciparum* under a jar with a candle lit to reduce the oxygen tension and increase the carbon dioxide tension that is essential for the parasite. This has led to the general view that reducing oxygen tension and increasing CO_2 to 5 % is beneficial for the parasites *in vitro.* Some researchers maintain the parasites at atmospheric oxygen levels and only increase the CO_2 concentration to 5%. However, this kind of oxidative assault had no impact on the parasite growth pattern that was observed under 1% and 20% oxygen tension. The Δ*gdha* trophozoites mature equally long as the wild type and the Δ*gdha* schizonts released the same number of merozoites regardless of the oxygen tension.

The exogenous stressor that was tested, t-BuOOH, was used to pronounce the oxidative challenge for the Δ*gdha* parasite line. The Δ*gdha* parasites could cope with the μM concentrations of the drug as well as the wild type parasites. Given these observations, it can be concluded that GDHa is not important for protection against external oxidative stresses.
The endogenous stressor tested, PMS, was intended to induce an oxidative stress in the parasite cell. Mutant and wild type parasites were shown to be equally sensitive to the stressor and the IC_{50} values are in the high nM range. Again these data suggest that GDHa is not prominently involved in an antioxidant defence. Given the hypothesis that GDHa provides the parasite cell with NADPH, this is rather a surprising result (Vander Jagt et al., 1989; Roth, 1990; Werner et al., 2005).

No substantial regulations of protein levels

Malaria parasite *P. falciparum* harbours enzymatic antioxidants such as superoxide dismutases and peroxiredoxins (Müller, 2004). These enzymes are backed up by enzymes that maintain the redox homeostasis of the cell. The parasite contains two redox systems: the thioredoxin and the glutathione system, both of which are dispensable for *P. berghei* but it remains to be verified that this can be transferred to *P. falciparum* (Pastrana-Mena et al., 2010; Buchholz et al., 2010). Two oxidoreductases, thioredoxin reductase and glutathione reductase, constitute a key link of either system (Müller, 2004). As both reductases are NADPH-specific, we hypothesized that they might be directly dependent on GDHa-mediated NADPH supply. Levels of glutathione reductase and thioredoxin were analysed here and no considerable up- or down-regulation of these two proteins was observed in Δ*gdha* mutant parasites as compared to wild type D10 parasites. This supports the notion that GDHa is unlikely to be involved in providing NADPH for reductive reactions. Obviously the regulation on protein level does not have to be necessarily connected to regulation of the relevant enzyme activities. That is something that needs to be addressed in future studies.

Slight up-regulations of gene transcripts

Gene expression regulation in the parasite is still largely unknown and the understanding of the regulatory mechanism lags far behind other eukaryotic systems. Previously thought, the gene transcription regulation was not under locus-specific promotor-based control (Deitsch et al., 2007). No general mechanism of transcriptional/translational regulation has been

established until ApiAP2 transcription factors were revealed (De Silva et al., 2008). ApiAP2 are proteins that contain AP2 DNA-binding domains homologous to already well characterized plant AP2 family of transcriptional regulators (Dietz et al., 2010). The current state of the field is that the parasite genes have their own upstream promoter sequences that are predominantly regulated transcriptionally. In the light of these findings, we proceeded to quantify the expression levels of genes that may be affected by a GDHa depletion by quantitative Real-Time PCR. We resorted to analysing the abundance of mRNA levels because no antibodies against these enzymes were available in the lab. The data suggest that there are no substantial changes in mRNA abundance *gdhb*, *gdhc*, *g6pd6pgl*, *γgcs*, and *gs*. The interpretation of these results and their actual biological importance is not straight forward. First, the ultimate gene function is expressed by a protein and it cannot be concluded that a twofold increase at transcript level necessarily leads to twofold increase of protein abundance. Second, the parasite undergoes rapid developmental changes on the molecular level (Otto et al., 2010). Due to the fact that we cannot distinguish through routine light microscopy examination the exact life stage of the parasite, it cannot be ruled out that samples contain a slightly different early/middle trophozoite ratios, i.e. slightly different transcript levels. Only higher-fold changes, in my opinion, should be considered as biologically important unless the quantitative Real-Time PCR is perfectly optimized and the source cell does not undergo rapid changes in their mRNA expression levels leading to marginal differences between the parasite lines. However, the fact that *g6pd6pgl* is not affected by GDHa depletion is in close agreement with observations of Atamna et al. (1994). In view of the fact that G6PDH activity is dependent on $NADP^+$/NADPH ratio, Atamna and colleagues (1994) tried to verify the role of GDH to maintain the reduced NADPH pool by comparing HMS activity of the parasites in presence or absence of glutamine or glutamate ethyl ester (which is hydrolysed to glutamate in the cell) but they did not observe any effect of either glutamine or glutamate ethyl ester addition on HMS activity suggesting that GDH is not involved in NADPH production (Atamna et al., 1994).

Increased GSH levels

Glutathione is important thiol redox buffer and a cofactor for redox active enzymes in the parasite cell (Müller et al., 2003). Glutathione levels change very sensitively in response to any sort of stress and its levels also change as the parasite matures. Consequently, it is very critical that the sample preparation is highly standardised so that changes in GSH level due to differences in parasite stages are accounted for. The GSH concentrations measured by

HPLC, as shown in this thesis, indicate clearly increasing levels in total GSH in the Δ*gdha* mutant parasites. These findings are in agreement with the slightly higher glutathione biosynthesis gene transcripts. Most importantly, this result is in agreement with a previous study of Roth and colleagues (1986) who noted that in normal infected red blood cells some glutathione disulphide is reduced by GDH. Given that we do not observe any other NADPH-producing enzymes up-regulation, GSSG that accumulates in the parasite may account for higher GSH levels in Δ*gdha* parasites.

Higher L-cycloserine susceptibility and controversial substrate preferences of GDHa *in vivo*

Glutamate represents a metabolic intercept of carbon and nitrogen metabolism of the cell (Aubert et al., 2001). Metabolic labelling of the parasites with [U-^{13}C]-glutamine did not show any differences in 2-oxoglutarate levels in Δ*gdha* mutants compared to wild type parasites (Dr Janet Storm, personal communication) suggesting that GDHa is either not responsible to generate the metabolite or that there is an alternative efficient way of generating 2-oxoglutarate in the mutant parasites. The only way to incorporate the five carbon skeleton of glutamate into 2-oxoglutarate is via aminotransferases (Fig. 20).

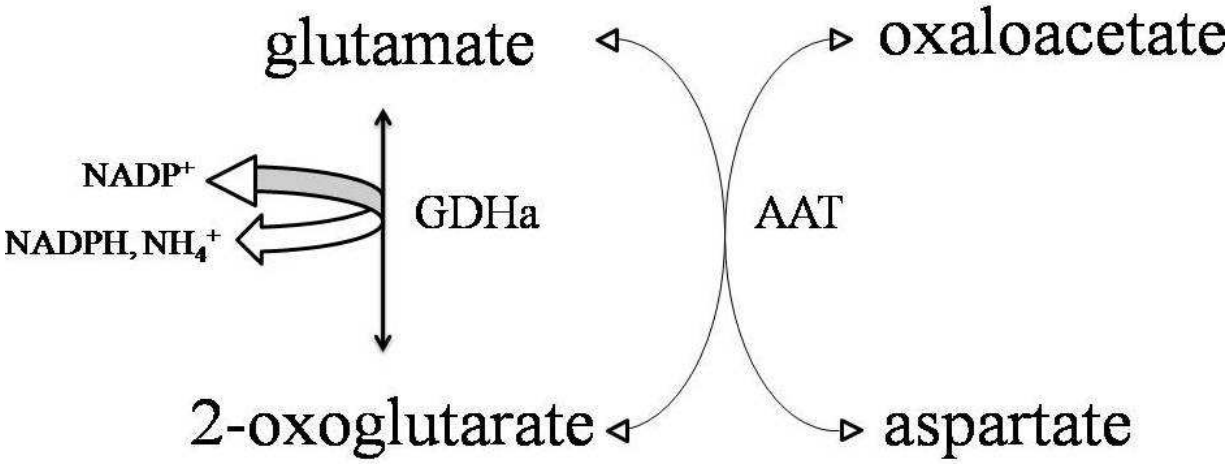

Figure 20. Scheme of glutamate deamination. Glutamate dehydrogenase a (GDHa) converts glutamate to 2-oxoglutarate and ammonia. The aspartate aminotransferase (AAT) transfers the amino group from glutamate to oxaloacetate with concomitant production of aspartate and 2-oxoglutarate. The reverse directions are also depicted.

Competition between the GDH and aminotransferases in glutamate deamination has been already described in plants (Aubert et al., 2001). In this context, we tried to selectively inhibit cellular aminotransferases to compare the sensitivity of wild type and mutant lines. The IC_{50} values clearly demonstrate a higher susceptibility of the Δ*gdha* mutant parasites to the inhibitor L-cycloserine and suggests that in the absence of GDHa, the carbon skeleton of

2-oxoglutarate for mitochondrial metabolism may be generated by an aminotransferase. *P. falciparum* encodes for three aminotransferases: aspartate aminotransferase (PFB0200c), ornithine aminotransferase (PFF0435w), and glucosamine-fructose-6-phosphate aminotransferase (PF10_0245). It is likely that one of the following two enzymes: aspartate aminotransferase (reaction scheme shown above) or ornithine aminotransferase (the glutamate-derived amino group is attached to proline instead of oxaloacetate and thus forming ornithine) are responsible for the conversion of glutamate into 2-oxoglutarate. As the L-cycloserine does not discriminate between aminotransferases regardless of concentration (Cornell et al., 1984), we cannot conclude at the moment which of the two aminotransferases takes over the catalytic step. To further discriminate between these two enzymes, we could have, for instance, measured the ammonia secreted in the medium as this only happens in the case of GDH catalysis and compare the media from wild type and mutant cell lines.

Furthermore, given the above results, one may suspect the previously suggested metabolic framework where *P. falciparum* GDHa favours the oxidative direction of the reaction being therefore favourably involved in generating glutamate through the reductive amination of 2-oxoglutarate (Vander Jagt et al., 1989). It may well be that the mM K_m for ammonia is not as restrictive as interpreted (Wagner et al., 1998). Incidentally, the findings of Vander Jagt and colleagues (1989) who noted that parasite GDH activity is about 12:1 in favour of glutamate synthesis cast first doubt on the hypothesis. In such a scenario, the knockout parasites would be overwhelmed with NADPH as it does not get used up in substitute aminotransferase catalysis. As a result, the inherent antioxidant defence of such a knockout would be of no lower efficiency. In some organisms, GDH works as an ammonia fixing enzyme which is further utilized in nitrogen requiring metabolism (Miflin and Habash, 2002). If true for *P. falciparum*, no striking phenotype could be seen due to generous amounts of glutamate and glutamine in RPMI 1640 complete medium. Both amino acids can be taken up by the parasite, plus glutamine can be converted, by glutamate synthase, to glutamate which is then available for the nitrogen metabolism. It is thus of highest importance to thoroughly revisit the catalytic properties of *P. falciparum* GDHa and set them in the cellular context.

Failure to generate Δ*gdhb* viable parasite line

GDHb is another potentially NADPH-producing enzyme. This enzyme was suggested to be localized in apicoplast of the parasite by Prof. Becker and colleagues (personal

correspondence). Because of the fact that the apicoplast metabolism is still not fully understood together with little information available for GDHb, it is quite difficult to infer any potential function of the enzyme in the organelle or elsewhere in the parasite. Nevertheless, the fact that no integration of either 3´ or 5´ end of the gene locus by the transfected gene replacement plasmid appeared after three rounds of off and on drug cycles may suggest a) the locus of the *gdhb* gene is not targetable and that is why the recombination is excluded. Such a suspicion would need a knock-in study to (dis)prove this hypothesis or b) the enzyme is essential or important for the parasite. If essential, no viable parasites can emerge upon deletion of the *gdhb* gene. If important, the absence of the enzyme lays such a heavy burden on the parasite that the knockout parasites get overgrown by wild type parasites in culture.

Conclusion

Overall, these findings do not support the previous concept that GDHa catalysis would be the main NADPH source for the parasite during intraerythrocytic growth. It was shown that GDHa deletion leads to viable stable parasite line with no growth defects. No enzymes or gene transcripts that are related to antioxidant defence or redox balance maintenance were shown to be down- or up-regulated in the knockout parasites. We reached some preliminary results indicating higher glutathione levels in the knockouts. The outputs from quantitative Real-Time PCR suggest that the two genes encoding the enzymes responsible for GSH biosynthesis appear to be slightly up-regulated which is in agreement with the finding that glutathione levels are increased in the mutant parasites. However, the data are not statistically significant because they show a great variability and need to be confirmed in future studies. In addition, it appeared that the Δ*gdha* mutant parasites show a higher sensitivity to the aminotransferases inhibitor L-cycloserine confirming the hypothesis of catalytic flexibility of this metabolic reaction. According to this study, it can be concluded that *P. falciparum* GDHa is not a suitable drug target for malaria treatment. The potential of GDHa as a promising drug target was also suspected by Crowther and colleagues (2011). This may, however, be different for GDHb as a gene deletion was impossible so far and it may be revealed in the future that this second GDH protein has vital functions for the malaria parasites.

5. References

Akerman SE, Müller S (2003) 2-Cys peroxiredoxin PfTrx-Px1 is involved in the antioxidant defence of *Plasmodium falciparum*. Mol Biochem Parasitol 130, 75–81.

Akoachere M, Iozef R, Rahlfs S, Deponte M, Mannervik B, Creighton DJ, Schirmer H, Becker K (2005) Characterization of the glyoxalases of the malarial parasite *Plasmodium falciparum* and comparison with their human counterparts. Biol Chem 386, 41–52.

Aparicio IM, Marín-Menéndez A, Bell A, Engel PC (2010) Susceptibility of *Plasmodium falciparum* to glutamate dehydrogenase inhibitors--a possible new antimalarial target. Mol Biochem Parasitol 172, 152–5.

Atamna H, Ginsburg H (1993) Origin of reactive oxygen species in erythrocytes infected with *Plasmodium falciparum*. Mol Biochem Parasitol 61, 231–41.

Atamna H, Pascarmona G, Ginsburg H (1994) Hexose-monophosphate shunt activity in intact *Plasmodium falciparum*-infected erythrocytes and in free parasites. Mol Biochem Parasitol 67, 79–89.

Aubert S, Bligny R, Douce R, Gout E, Ratcliffe RG, Roberts JK (2001) Contribution of glutamate dehydrogenase to mitochondrial glutamate metabolism studied by (13)C and (31)P nuclear magnetic resonance. J Exp Bot 52, 37–45.

Bernroitner M, Zamocky M, Furtmüller PG, Peschek GA, Obinger C (2009) Occurrence, phylogeny, structure, and function of catalases and peroxidases in cyanobacteria. J Exp Bot 60, 423–40.

Boucher IW, McMillan PJ, Gabrielsen M, Akerman SE, Brannigan JA, Schnick C, Brzozowski AM, Wilkinson AJ, Müller S (2006) Structural and biochemical characterization of a mitochondrial peroxiredoxin from *Plasmodium falciparum*. Mol Microbiol 61, 948–59.

Buchholz K, Putrianti ED, Rahlfs S, Schirmer RH, Becker K, Matuschewski K (2010) Molecular genetics evidence for the *in vivo* roles of the two major NADPH-dependent disulfide reductases in the malaria parasite. J Biol Chem 285, 17388–95.

Clarke JL, Scopes DA, Sodeinde O, Mason PJ (2001) Glucose-6-phosphate dehydrogenase-6-phosphogluconolactonase. A novel bifunctional enzyme in malaria parasites. Eur J Biochem 268, 2013–9.

Cobbold SA, Martin RE, Kirk K (2011) Methionine transport in the malaria parasite *Plasmodium falciparum*. Int J Parasitol 41, 125–35.

Cornell NW, Zuurendonk PF, Kerich MJ, Straight CB (1984) Selective inhibition of alanine aminotransferase and aspartate aminotransferase in rat hepatocytes. Biochem J 202, 707–16.

Crowther GJ, Napuli AJ, Gilligan JH, Gagaring K, Borboa R, Francek C, Chen Z, Dagostino EF, Stockmyer JB, Wang Y, Rodenbough PP, Castaneda LJ, Leibly DJ, Bhandari J, Gelb MH, Brinker A, Engels IH, Taylor J, Chatterjee AK, Fantauzzi P, Glynne RJ, Van Voorhis WC, Kuhen KL (2011) Identification of inhibitors for putative malaria drug targets among novel antimalarial compounds. Mol Biochem Parasitol 175, 21–9.

Deitsch K, Duraisingh M, Dzikowski R, Gunasekera A, Khan S, Le Roch K, Llinás M, Mair G, McGovern V, Roos D, Shock J, Sims J, Wiegand R, Winzeler E (2007) Mechanisms of gene regulation in *Plasmodium*. Am J Trop Med Hyg 77, 201–8.

de Koning-Ward TF, Gilson PR, Boddey JA, Rug M, Smith BJ, Papenfuss AT, Sanders PR, Lundie RJ, Maier AG, Cowman AF, Crabb BS (2009) A newly discovered protein export machine in malaria parasites. Nature 459, 945–9.

De Silva EK, Gehrke AR, Olszewski K, León I, Chahal JS, Bulyk ML, Llinás M (2008) Specific DNA-binding by apicomplexan AP2 transcription factors. Proc Natl Acad Sci USA 105, 8393–8.

Dietz KJ, Vogel MO, Viehhauser A (2010) AP2/EREBP transcription factors are part of gene regulatory networks and integrate metabolic, hormonal and environmental signals in stress acclimation and retrograde signalling. Protoplasma 245, 3–14.

Eckman JR, Eaton JW (1979) Dependence of plasmodial glutathione metabolism on the host cell. Nature 278, 754–6.

Egan TJ, Combrinck JM, Egan J, Hearne GR, Marques HM, Ntenteni S, Sewell BT, Smith PJ, Taylor D, van Schalkwyk DA, Walden JC (2002) Fate of haem iron in the malaria parasite *Plasmodium falciparum*. Biochem J 365, 343–7.

Foth BJ, Stimmler LM, Handman E, Crabb BS, Hodder AN, McFadden GI (2005) The malaria parasite *Plasmodium falciparum* has only one pyruvate dehydrogenase complex, which is located in the apicoplast. Mol Microbiol 55, 39–53.

Friedman MJ (1979) Oxidant damage mediates variant red cell resistance to malaria. Nature 280, 245–7.

Ginsburg H (2002) Abundant proton pumping in *Plasmodium falciparum*, but why? Trends Parasitol 18, 483–6.

Ginsburg H (2009) Caveat emptor: limitations of the automated reconstruction of metabolic pathways in *Plasmodium*. Trends Parasitol 25, 37–43.

Gueirard P, Tavares J, Thiberge S, Bernex F, Ishino T, Milon G, Franke-Fayard B, Janse CJ, Ménard R, Amino R (2010) Development of the malaria parasite in the skin of the mammalian host. Proc Natl Acad Sci USA 107, 18640–5.

Günther S, McMillan PJ, Wallace LJ, Müller S (2005) *Plasmodium falciparum* possesses organelle-specific alpha-keto acid dehydrogenase complexes and lipoylation pathways. Biochem Soc Trans 33, 977–80.

Günther S, Wallace L, Patzewitz EM, McMillan PJ, Storm J, Wrenger C, Bissett R, Smith TK, Müller S (2007) Apicoplast lipoic acid protein ligase B is not essential for *Plasmodium falciparum*. PLoS Pathog 3:e189.

Günther S, Matuschewski K, Müller S (2009a) Knockout studies reveal an important role of *Plasmodium* lipoic acid protein ligase A1 for asexual blood stage parasite survival. PLoS Pathog 4:e5510.

Günther S, Storm J, Müller S (2009b) *Plasmodium falciparum*: organelle-specific acquisition of lipoic acid. Int J Biochem Cell Biol 41, 748–51.

Harper CJ, Hayward D, Kidd M, Wiid I, van Helden P (2010) Glutamate dehydrogenase and glutamine synthetase are regulated in response to nitrogen availability in *Myocbacterium smegmatis*. BMC Microbiol 10:138.

Hay SI, Okiro EA, Gething PW, Patil AP, Tatem AJ, Guerra CA, Snow RW (2010) Estimating the global clinical burden of *Plasmodium falciparum* malaria in 2007. PLoS Med 7:e1000290.

Hunt NH, Stocker R (1990) Oxidative stress and the redox status of malaria-infected erythrocytes. Blood Cells 16, 499–526.

Jortzik E, Mailu BM, Preuss J, Fischer M, Bode L, Rahlfs S, Becker K (2011) Glucose 6-phosphate dehydrogenase 6-phosphogluconolactonase: a unique bifunctional enzyme from *Plasmodium falciparum*. Biochem J [in press; doi:10.1042/BJ20110170].

Kawazu S, Tsuji N, Hatabu T, Kawai S, Matsumoto Y, Kano S (2000) Molecular cloning and characterization of a peroxiredoxin from the human malaria parasite *Plasmodium falciparum*. Mol Biochem Parasitol 109, 165–9.

Kehr S, Sturm N, Rahlfs S, Przyborski JM, Becker K (2010) Compartmentation of redox metabolism in malaria parasites. PLoS Pathog 6:e1001242.

Krauth-Siegel RL, Müller JG, Lottspeich F, Schirmer RH (1996) Glutathione reductase and glutamate dehydrogenase of *Plasmodium falciparum*, the causative agent of tropical malaria. Eur J Biochem 235, 345–50.

Kuehn A, Pradel G (2010) The coming-out of malaria gametocytes. J Biomed Biotechnol 2010:976827.

Kwatia MA, Botkin DJ, Williams DL (2000) Molecular and enzymatic characterization of *Schistosoma mansoni* thioredoxin peroxidase. J Parasitol 86, 908–15.

Lane N (2002) Oxygen. Oxford University Press, New York.

Lian LY, Al-Helal M, Roslaini AM, Fisher N, Bray PG, Ward SA, Biagini GA (2009) Glycerol: an unexpected major metabolite of energy metabolism by the human malaria parasite. Malaria J 8:38.

Ling IT, Wilson RJ (1988) Glucose-6-phosphate dehydrogenase activity of the malaria parasite *Plasmodium falciparum*. Mol Biochem Parasitol 31, 47–56.

Loria P, Miller S, Foley M, Tilley L (1999) Inhibition of the peroxidative degradation of haem as the basis of action of chloroquine and other quinoline antimalarials. Biochem J 339, 363–70.

Low FM, Hampton MB, Peskin AV, Winterbourn CC (2007) Peroxiredoxin 2 functions as a noncatalytic scavenger of low-level hydrogen peroxide in the erythrocyte. Blood 109, 2611–7.

Manta B, Hugo M, Ortiz C, Ferrer-Sueta G, Trujillo M, Denicola A (2009) The peroxidase and peroxynitrite reductase activity of human erythrocyte peroxiredoxin 2. Arch Biochem Biophys 484, 146–54.

McGonigle S, Curley GP, Dalton JP (1997) Cloning of peroxiredoxin, a novel antioxidant enzyme, from the helminth parasite *Fasciola hepatica*. Parasitology 115, 101–4.

Mercer-Haines N, Fioravanti CF (2008) *Hymenolepis diminuta*: mitochondrial transhydrogenase as an additional site for anaerobic phosphorylation. Exp Parasitol 119, 24–9.

Miflin BJ, Habash DZ (2002) The role of glutamine synthetase and glutamate dehydrogenase in nitrogen assimilation and possibilities for improvement in the nitrogen utilization of crops. J Exp Bot 53, 979–87.

Mogi T, Kita K (2010) Diversity in mitochondrial metabolic pathways in parasitic protists *Plasmodium* and *Cryptosporidium*. Parasitol Int 59, 305–12.

Müller S, Liebau E, Walter RD, Krauth-Siegel RL (2003) Thiol-based redox metabolism of protozoan parasites. Trends Parasitol 19, 320–8.

Müller S (2004) Redox and antioxidant systems of the malaria parasite *Plasmodium falciparum*. Mol Microbiol 53, 1291–305.

Olszewski KL, Mather MW, Morrisey JM, Garcia BA, Vaidya AB, Rabinowitz JD, Llinás M (2010) Branched tricarboxylic acid metabolism in *Plasmodium falciparum*. Nature 466, 744–8.

Otto TD, Wilinski D, Assefa S, Keane TM, Sarry LR, Böhme U, Lemieux J, Barrell B, Pain A, Berriman M, Newbold C, Llinás M (2010) New insights into the blood-stage transcriptome of *Plasmodium falciparum* using RNA-Seq. Mol Microbiol 76, 12–24.

Pastrana-Mena R, Dinglasan RR, Franke-Fayard B, Vega-Rodríguez J, Fuentes-Caraballo M, Baerga-Ortiz A, Coppens I, Jacobs-Lorena M, Janse CJ, Serrano AE (2010) Glutathione reductase-null malaria parasites have normal blood stage growth but arrest during development in the mosquito. J Biol Chem 285, 27045–56.

Pei Y, Tarun AS, Vaughan AM, Herman RW, Soliman JM, Erickson-Wayman A, Kappe SH (2010) *Plasmodium* pyruvate dehydrogenase activity is only essential for the parasite's progression from liver infection to blood infection. Mol Microbiol 75, 957–71.

Peters AL, Van Noorden CJ (2009) Glucose-6-phosphate dehydrogenase deficiency and malaria: cytochemical detection of heterozygous G6PD deficiency in women. J Histochem Cytochem 57, 1003–11.

Pino P, Foth BJ, Kwok LY, Sheiner L, Schepers R, Soldati T, Soldati-Favre D (2007) Dual targeting of antioxidant and metabolic enzymes to the mitochondrion and the apicoplast of *Toxoplasma gondii*. PLoS Pathog 3:e115.

Plaitakis A, Zaganas I (2001) Regulation of human glutamate dehydrogenases: implications for glutamate, ammonia and energy metabolism in brain. J Neurosci Res 66, 899–908.

Purnell MP, Botella JR (2007) Tobacco isoenzyme 1 of NAD(H)-dependent glutamate dehydrogenase catabolizes glutamate *in vivo*. Plant Physiol 143, 530–9.

Radfar A, Méndez D, Moneriz C, Linares M, Marín-García P, Puyet A, Diez A, Bautista JM (2009) Synchronous culture of *Plasmodium falciparum* at high parasitemia levels. Nat Protoc 4, 1899–915.

Richard D, Bartfai R, Volz J, Ralph SA, Muller S, Stunnenberg HG, Cowman AF (2011) A Genome-wide Chromatin-associated Nuclear Peroxiredoxin from the Malaria Parasite *Plasmodium falciparum*. J Biol Chem 286, 11746–55.

Roth EF Jr, Raventos-Suarez C, Rinaldi A, Nagel RL (1983) Glucose-6-phosphate dehydrogenase deficiency inhibits in vitro growth of *Plasmodium falciparum*. Proc Natl Acad Sci USA 80, 298–9.

Roth EF Jr., Schulman S, Vanderberg J, Olson J (1986) Pathways for the reduction of oxidized glutathione in the *Plasmodium falciparum*-infected erythrocyte: can parasite enzymes replace host red cell glucose-6-phosphate dehydrogenase? Blood 67, 827–30.

Roth E Jr (1990) *Plasmodium falciparum* carbohydrate metabolism: a connection between host cell and parasite. Blood Cells 16, 453–60.

Salanti A, Staalsoe T, Lavstsen T, Jensen AT, Sowa MP, Arnot DE, Hviid L, Theander TG (2003) Selective upregulation of a single distinctly structured var gene in chondroitin sulphate A-adhering *Plasmodium falciparum* involved in pregnancy-associated malaria. Mol Microbiol 49, 179–91.

Schall JJ (1989) The sex ratio of Plasmodium gametocytes. Parasitology 98, 343–50.

Seeber F, Soldati-Favre D (2010) Metabolic Pathways in the Apicoplast of Apicomplexa. Int Rev Cell Moll Biol 281, 161–228.

Sherman IW (1979) Biochemistry of *Plasmodium* (malarial parasites). Microbiol Rev 43, 453–95.

Sienkiewicz N, Daher W, Dive D, Wrenger C, Viscogliosi E, Wintjens R, Jouin H, Capron M, Müller S, Khalife J (2004) Identification of a mitochondrial superoxide dismutase with an unusual targeting sequence in *Plasmodium falciparum*. Mol Biochem Parasitol 137, 121–32.

Slater AF, Cerami A (1992) Inhibition by chloroquine of a novel haem polymerase enzyme activity in malaria trophozoites. Nature 355, 167–9.

Trager W, Jensen JB (1976) Human malaria parasites in continuous culture. Science 193, 673–5.

Turrens JF (2004) Oxidative stress and antioxidant defenses: a target for the treatment of diseases caused by parasitic protozoa. Mol Aspects Med 25, 211–20.

Usanga EA, Luzzatto L (1985) Adaptation of Plasmodium falciparum to glucose 6-phosphate dehydrogenase-deficient host red cells by production of parasite-encoded enzyme. Nature 313, 793–5.

Vander Jagt DL, Intress C, Heidrich JE, Mrema JE, Rieckmann KH, Heidrich HG (1982) Marker enzymes of *Plasmodium falciparum* and human erythrocytes as indicators of parasite purity. J Parasitol 68, 1068–71.

Vander Jagt DL, Hunsaker LA, Kibirige M, Campos NM (1989) NADPH production by the malarial parasite *Plasmodium falciparum*. Blood 74, 471–74.

van Dooren GG, Stimmler LM, McFadden GI (2006) Metabolic maps and functions of the *Plasmodium* mitochondrion. FEMS Microbiol Rev 30, 596–630.

Wagner JT, Lüdemann H, Färber PM, Lottspeich F, Krauth-Siegel RL (1998) Glutamate dehydrogenase, the marker protein of *Plasmodium falciparum*--cloning, expression and characterization of the malarial enzyme. Eur J Biochem 258, 813–9.

Werner C, Stubbs MT, Krauth-Siegel RL, Klebe G (2005) The crystal structure of *Plasmodium falciparum* glutamate dehydrogenase, a putative target for novel antimalarial drugs. J Mol Biol 349, 597–607.

Wilkinson SR, Temperton NJ, Mondragon A, Kelly JM (2000) Distinct mitochondrial and cytosolic enzymes mediate trypanothione-dependent peroxide metabolism in *Trypanosoma cruzi*. J Biol Chem 275, 8220–5.

Williams RA, Westrop GD, Coombs GH (2009) Two pathways for cysteine biosynthesis in *Leishmania major*. Biochem J 420, 451–62.

Yano K, Otsuki H, Arai M, Komaki-Yasuda K, Tsuboi T, Torii M, Kano S, Kawazu S (2008) Disruption of the *Plasmodium berghei* 2-Cys peroxiredoxin TPx-1 gene hinders the sporozoite development in the vector mosquito. Mol Biochem Parasitol 159, 142–5.

Yoshida A, Roth EF Jr. (1987) Glucose-6-phosphate dehydrogenase of malaria parasite *Plasmodium falciparum*. Blood 69, 1528–30.

Zerez CR, Lachant NA, Lee SJ, Tanaka KR (1988) Decreased erythrocyte nicotinamide adenine dinucleotide redox potential and abnormal pyridine nucleotide content in sickle cell disease. Blood 71, 512–5.